Delft University of Technology
Master of Science Thesis in Embedded Systems

Screen Antenna: Integrated Data Transfer and Display using RGB LEDs

Nishad Mandlik

TU Delft Delft University of Technology

Screen Antenna: Integrated Data Transfer and Display using RGB LEDs

Master of Science Thesis in Embedded Systems

Embedded Systems Group
Faculty of Electrical Engineering, Mathematics and Computer Science
Delft University of Technology
Van Mourik Broekmanweg 6, 2628 XE Delft, The Netherlands

Nishad Mandlik

02 July 2023

Author
Nishad Mandlik

Title
Screen Antenna: Integrated Data Transfer and Display using RGB LEDs

MSc Presentation Date
06 July 2023

Graduation Committee

Dr. Marco Zúñiga	Delft University of Technology
Dr. Qing Wang	Delft University of Technology

Abstract

This thesis presents Screen Antenna - A Visible Light Communication (VLC) system that integrates data transmission and reception, with the conventional pixel display capability of RGB LEDs. The system is constructed with off-the-shelf components and runs on the Arduino Due microcontroller. The hardware and software have been designed with the objectives of scalability and flexibility. This research aims to optimize the system's performance in terms of throughput, error rate, and display quality.

To evaluate the system's performance, extensive experiments were conducted under different lighting conditions, PWM frequency and Rx-Tx distances. The experiments focused on achieving the maximum achievable throughput while maintaining a low Bit Error Rate (BER). Through careful optimization of the system parameters, a maximum throughput of 4.4kbps was achieved. Furthermore, the system consistently maintained a Bit Error Rate of less than 0.005%, ensuring reliable and error-free data transmission.

In addition to data transmission, the impact of data transmission on the display's visual quality was investigated. The Delta E value, which quantifies the observed colour difference between two pixel values, was used as a metric for display quality. The data rates were calibrated such that the display operated with a Delta-E value of less than 1 in more than 90% of the colour spectrum, indicating minimal colour distortion during data transmission.

This study contributes to the field of VLC by showcasing a practical implementation that combines scalability, visual quality, and performance. Future research directions could focus on expanding the display size and enhancing the data rate by means of more sophisticated hardware.

"Science is about knowing, engineering is about doing." – Henry Petroski

Preface

The idea for this thesis emerged from discussions between me and my supervisor, Dr. Qing Wang. I was intrigued by the photo-sensing abilities of LEDs and decided to exploit this ability to develop LED displays that are capable of data transmission. The course of this project with the Embedded Systems group at TU Delft has been challenging, which enabled me to enhance my skills in areas such as embedded software, hardware communication, 3D printing, and most importantly, hand-soldering SMD components.

I would like to express my sincere gratitude to my supervisor, Dr. Qing Wang, for his unwavering support and invaluable guidance throughout this research endeavor. His expertise and enthusiasm for Visible Light Communication have been instrumental in shaping the direction of this thesis project. His constructive feedback has played a pivotal role in refining the research methodology and achieving meaningful results. I would also like to extend my appreciation to Ran Zhu, a PhD candidate at TU Delft for helping me with the availability of several hardware components that I needed at various stages of this project. Furthermore, I would like to acknowledge the contribution of RoboISM - The Robotics Club of IIT (ISM) Dhanbad in shaping my skill set and inculcating in me, an interest in embedded systems. Finally, I am grateful to my family and friends for their encouragement, understanding, and belief in my abilities throughout this journey. Their support has been a constant source of motivation and inspiration.

Nishad Mandlik

Delft, The Netherlands
2nd July 2023

Contents

Chapter 1

Introduction

In an era characterized by ever-increasing connectivity and information exchange, the demand for fast, reliable, and secure wireless communication technologies has become paramount. Traditional methods, such as radio frequency (RF) and microwave-based communication, have played a vital role in shaping our interconnected world. However, the growing scarcity of RF spectrum [1] and concerns regarding data security have paved the way for an emerging technology with immense potential — Visible Light Communication (VLC) [14]. Furthermore, VLC is immune to electromagnetic interference, making it a reliable option in environments where radio frequency interference may be an issue [14]. Finally, VLC can be integrated with the existing light-emitting devices, allowing for dual functionality in the same system.

LEDs are widely used for illumination and display. With the advent of VLC, the use of LEDs as data transmitters is gaining popularity. Furthermore, inorganic LEDs can also sense light to a certain extent due to their inherent photodiode-like properties [6]. Under reverse bias, these LEDs exhibit the potential to be operated in the photovoltaic mode. When photons with sufficient energy (greater than the bandgap energy of the semiconductor material) strike the LED, they can generate electron-hole pairs within the depletion region of the LED. This creates a potential difference, which can be measured as a voltage or used to drive a current flow. By measuring the resulting voltage or current, the intensity or presence of light can be inferred. However, it is important to note that the photovoltaic functionality of LEDs is not as optimized as that of dedicated photodiodes. LEDs are primarily designed for efficient light emission, so their sensitivity as light detectors may be relatively lower compared to specialized photodiodes. Nonetheless, in certain situations where both light emission and detection are desired, inorganic LEDs can serve the dual purpose of emitting and sensing light [6].

In the realm of consumer electronics, LED displays are prominently featured in televisions, smartphones, laptops, and smartwatches, offering vivid colours, high contrast ratios, and energy efficiency. LED displays have also become the go-to choice for digital signage, both indoors and outdoors, due to their superior brightness, visibility in different lighting conditions, and ability to create large-scale, eye-catching displays. The development of LED technology has played a significant role in the advancement of display technology. The timeline starts with the development of the first LED matrix display in 1968. These early

LED displays utilized classic inorganic LEDs [15]. However, one limitation of these LEDs was that they could not be reduced in size, which affected the pixel density and overall resolution of the display. This limitation was overcome with the development of Passive Matrix Organic LEDs (PMOLEDs). PMOLED displays offered improved pixel density and resolution compared to classic inorganic LEDs. However, they were associated with certain drawbacks, including a shorter lifetime and scalability issues [2]. The shorter lifetime meant that the OLED pixels would degrade over time, leading to a reduction in display quality and eventually, the need for replacement. Subsequently, Active Matrix Organic LEDs (AMOLEDs) were introduced as a solution to the scalability problems faced by PMOLEDs. AMOLED displays allowed for better scalability which made them suitable for applications such as televisions and large displays [2]. However, the lifetime limitation of OLED technology still persisted with AMOLEDs. Now, a promising development in the field of display technology is the emergence of microLEDs. MicroLEDs are essentially micro-scale inorganic LEDs, thus offering a longer lifetime along with small-size advantages. This means that microLED displays can achieve higher pixel density, improved resolution, and longer lifetimes compared to previous technologies [4]. It is important to realise that while microLEDs show great promise, they are still in the development phase and have not yet been widely commercialized. However, ongoing research and advancements in microLED technology suggest a potential breakthrough in the display industry in the future.

1.1 Problem Statement

With inorganic LEDs being the future of display technology, and their ability to transmit and receive data, we aim to design RGB-LED displays that are capable of data transfer without any additional photo-sensor (Figure 1.1). While LED displays excel in visual output, their current design primarily focuses on one-way information dissemination, hindering their potential for interactive data exchange. This limitation creates a demand for a solution that enables bidirectional data transfer within LED displays, facilitating real-time interactivity.

1.2 Challenges

The integration of data transfer capabilities into an RGB LED Display comes with several challenges:

1. **Photo-sensitivity**
   The first hurdle involves obtaining a substantial output from the LED when used as a light sensor. As LEDs are primarily designed for light emission rather than light detection, their inherent sensitivity in the photovoltaic is relatively lower. This necessitates the incorporation of appropriate amplification circuitry to enhance their sensitivity for accurate photodetection.

2. **Mode switching**
   The system needed to seamlessly switch between multiple modes of operation, namely display, transmit, and receive. This necessitates the inclusion

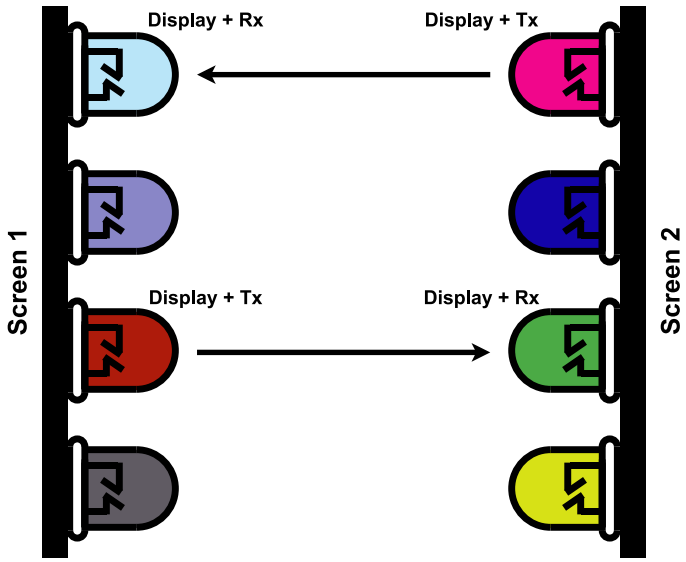

Figure 1.1: **Concept of the Screen Antenna System**

of switching components within the circuit design. When the LED is emitting light, it operates in forward bias, whereas as a light sensor, it requires reverse bias. Hence, switching components are needed in the circuit to facilitate these requirements. Secondly, due to conflicting bias requirements, simultaneous display and reception are not possible. As a workaround to this limitation, the LED's Pulse Width Modulation (PWM) cycle needs to be leveraged to perform data reception during the off-time of the display cycle. Furthermore, on the software side, efficient time-sharing implementation is crucial for the processor to handle the dual responsibilities of data transfer and refreshing pixels.

3. **Visual Quality**
   Displaying pixels is still the primary purpose of the screen. Hence, data transfer algorithms should be designed such that the visual quality of the content displayed on the screen is not compromised.

1.3 Contributions

The notable contributions introduced by this thesis are as outlined below:

1. **Utilization of Off-the-Shelf Components**
   The project leveraged readily available off-the-shelf components to build 4x4 RGB LED displays, making them accessible for implementation in various applications and reducing the need for custom-designed components, thereby saving time and resources.

2. **Increasing throughput without compromising on pixel quality**
   Both display and transmission require the LED to emit light. Operating these two functions with Time Division Multiplexing (TDM) causes mutual influence, thus hampering the performance of both. A logical step is

to intertwine these together into one function. This is accomplished by superimposing phase shifts with the PWM signal. While the duty cycle is responsible for displaying the desired pixel colour, phase modulation is used to transmit different bit values (0 and 1). Thus, the pixel colour limits the maximum achievable data rate. In view of this, we propose an algorithm that allows us to maximize the duty cycle while ensuring that the colour difference is below the differentiation threshold of human vision. Moreover, this project also presents the use of multiple transmitter LEDs with a single receiver, to ensure that the available cycle is used to the fullest.

3. **Initial Scanning for Potential Transmitters**
   As mentioned above, a receiver LED needs to receive data from multiple transmitter LEDs. But due to geometrical inaccuracies in the displays, these cannot be statically assigned. Hence, an initial scanning phase is incorporated into the system to dynamically identify potential transmitters for each receiver LED.

4. **Immunity to Lighting Conditions**
   The system uses relative values of light intensity which makes it operable in a wide range of lighting conditions, following an initial calibration.

1.4 Organization

The organization of this report follows the development process of the project. First, some related works are introduced, to provide a background of this field and pave the way for commencing this project. Next, we give a brief overview of the system. This is followed by the hardware architecture of the system which forms the basis for the subsequent software implementation. With the basic functionality implemented, we move forward to describe a couple of techniques (Colour Augmentation and Many-to-One Communication) to improve the data-rate of the system. Then, the report presents the results of evaluating the system under different test conditions. And finally, the conclusion and future scope for research are discussed.

Chapter 2

Related Work

2.1 Visible Light Communication (VLC)

Visible Light Communication (VLC) is a wireless communication technology that utilizes visible light for data transmission. It leverages the properties of light, particularly the rapid switching capabilities of Light-Emitting Diodes (LEDs), to enable high-speed and secure data communication.

VLC works by modulating the intensity of light emitted by LEDs at a speed that is imperceptible to the human eye. These light-intensity variations carry digital information in the form of data bits. The modulation techniques commonly used in VLC include on-off keying (OOK), pulse amplitude modulation (PAM), and frequency shift keying (FSK).

To establish a VLC link, a transmitting device encodes data into light signals by rapidly turning the LED on and off or adjusting its brightness. The light signals are then detected and decoded by a light sensor, at the receiving end. The sensor converts the received light into electrical signals, which are further processed and interpreted as data.

VLC does have some limitations, including the need for a direct line of sight, limited coverage range, and sensitivity to ambient lighting conditions. However, ongoing advancements in VLC technology, along with its unique advantages, continue to expand its potential applications and make it an increasingly promising wireless communication solution.

2.2 Light Sources

A light source is necessary for transmitting data in VLC. VLC focuses on integrating data transmission capabilities into the existing illumination infrastructure. Data modulation is performed directly at the light source, or by using modulators such as polarisers and liquid crystals in conjunction with a light source. LEDs, LASER Diodes or even sunlight can act as potential sources for VLC. Research on using LEDs as data transmitters has gained significant attention in recent years due to its potential applications in various fields. This technology utilizes the rapid switching capabilities of LEDs to transmit data through light signals. Various studies have been conducted to explore the potential of LED-based data transmission. These studies have focused on areas

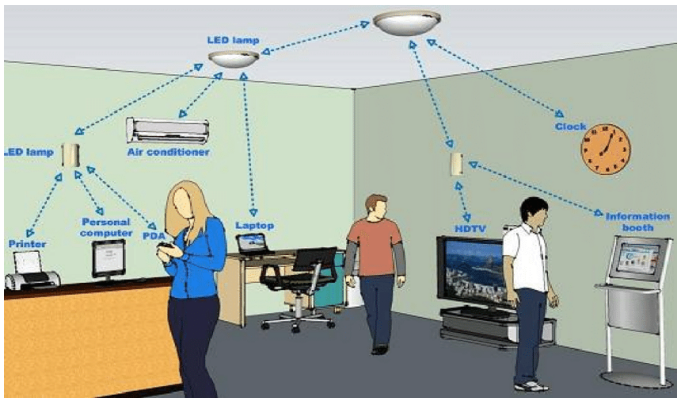

Figure 2.1: **Potential applications of Visible Light Communication (Source: [8])**

such as modulation techniques, receiver design, channel characteristics, and system performance.

2.3 Light Sensors

VLC utilizes light sensors to detect light signals for data reception. Selection of a light sensor depends on the specific requirements of the VLC system, including the desired data rate, transmission distance, ambient light conditions, and cost considerations. Some examples of such sensors are listed below:

1. **Light-dependent Resistor (LDR)**
   LDRs are passive components that exhibit a change in resistance based on the intensity of incident light. They are commonly used in various light-sensing applications, but due to their lower sensitivity and slower response times, they are not suitable for data communication.

2. **Photodiode and Phototransistor**
   These light-sensing devices are widely used in VLC. They work on the principle of Photoelectric Effect and generate a current when excited by incoming photons.

3. **Image Sensor**
   In applications where imaging devices such as cameras act as VLC receivers, the light sensing is performed by Complementary Metal-Oxide-Semiconductor (CMOS) or Charge-Coupled Device (CCD) based image sensors.

4. **Photomultiplier Tube (PMT)**
   PMTs are highly sensitive light detectors that can amplify very weak light signals. They consist of a photocathode, electron multiplier stages, and an anode. PMTs are primarily used in specialized VLC applications that require extremely high sensitivity, such as low-light conditions or long-range communications.

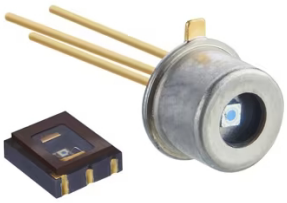

(a) **Photodiode (Source: [5])**

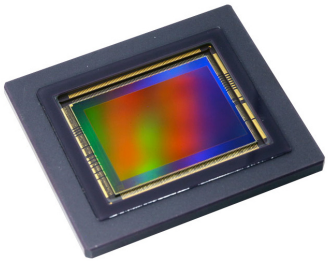

(b) **CMOS Sensor (Source: [19])**

(c) **PMT (Source: [7])**

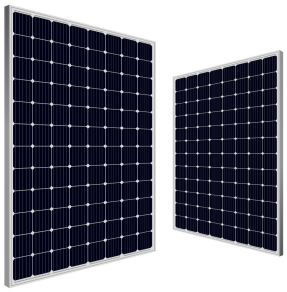

(d) **Solar Panel (Source: [22])**

(e) **LED (Source: [24])**

Figure 2.2: **Some of the light sensors that are used as data receivers in VLC**

5. **Solar Cell**
   In addition to harvesting energy from sunlight, solar cells have also found applications as light sensors, in the field of VLC. The use of a solar panel as a data receiver has been demonstrated in [20].

6. **Light Emitting Diode (LED)**
   LEDs bear several similarities with photodiodes in terms of structure and band-gap. Research has explored the innovative use of LEDs as sensors, expanding their capabilities beyond traditional lighting applic-

ations. LEDs have demonstrated the potential to serve as cost-effective and versatile sensors in various fields.

2.4 LED-to-LED Data Transfer Without Lighting Constraints

Initial works on using LEDs for data communication date back to as early as 2003. Dietz et al. [2003] presents a nascent technique for establishing bidirectional data transfer between two LEDs directed towards each other. It uses "Morse code"-like symbols to represent '0' and '1' bits and the message protocol is similar to the RS-232 standard. However, in this study, LEDs were only used for transferring data, without having any primary functionality. Thus, the LEDs did not have any requirements to maintain a specified intensity or to be flicker-free.

Schmid et al. [2013] discusses the creation of ad-hoc networks using red LEDs positioned in a circular arrangement. Further works, namely Chun et al. [2014] and Stepniak et al. [2015] are aimed at increasing the throughput of the LED-to-LED communication beyond 100Mbps. This has been achieved through the use of transimpedance amplifiers, LEDs with a larger emission and detection area, and the implementation of better modulation schemes such as Orthogonal frequency-division multiplexing (OFDM) and Discrete Multi-Tone (DMT) Modulation. Studies such as Kadirvelu and B [2017] are focused on the use of high-pass filters for increasing the immunity of the LED communication system towards ambient light. The performance of various coloured LEDs in communication has been explored in Umrani et al. [2018]. Still, in all these works, LEDs were solely used for the purpose of transmitting and receiving data, and therefore, had no constraints on their lighting properties. More recently, Mir et al. [2022] provided a step in this direction. It uses RGB LEDs to perform various functions. Based on the transmission and reception properties of the red, green, and blue components, it uses the red colour for transmission, and blue and green for illumination and sensing of environmental parameters.

2.5 LED-to-LED Data Transfer With Lighting Constraints

The work presented in Li et al. [2017] bares several similarities to the goal of this thesis. It proposes data transmission architecture and modulation schemes for communication between two LEDs whose primary functionality is illumination. Techniques for transmission and reception while maintaining the LEDs at a desired brightness are discussed. The transmitter or the receiver, however, uses a single LED, or a group of LEDs that operate synchronously at the same intensity. Hence, it fails to provide the architecture for managing several LEDs which have to operate at different intensities.

Some later developments in this area have concentrated on devising modulation schemes for LED transmitters. Henao et al. [2019] and Henao-Rios et al. [2020] present modulation techniques that enable LEDs to perform the dual functionality of illumination and data transmission. These techniques en-

sure that the data is transmitted in such a way that the intended illumination is sustained. Yet, these studies use LEDs only for transmission, while the reception is performed by dedicated photo-sensors. When LEDs have to be used as sensors, their dual functionality restricts their capabilities to sample the received signal. This factor needs to be taken into account while choosing a modulation scheme for LED-to-LED communication.

2.6 Touch Screen

LEDs have been explored for proximity sensing. By utilizing their light emission and detection capabilities, LEDs can identify the presence and movement of objects in their vicinity. In Hönck [2011], a red LED display with touch screen functionality is presented. At a given instant, some of the LEDs in the matrix are *ON* and the others are *OFF*. The *OFF* are used to sense the light reflected from the *ON* LEDs. Reflections occur when an object is placed in close proximity to the LED matrix. This is how the "touch" functionality is emulated. The concept used is similar to this thesis in the sense that the LED matrix is capable of simultaneous display, transmission, and reception. However, the touch-screen application misses a few key features that are required for our Screen Antenna system. Firstly, the touch screen uses only red LEDs instead of the RGB ones. This means that the design complexity is less, and also displaying a multi-coloured content is not possible. Secondly, the receiver LED only needs to detect the presence or absence of reflected light. Thus, accurate decoding of data is not required. And finally, LEDs in the touch screen are only operated as *ON* or *OFF*, without having any intensity variation. The goal of this thesis is to implement elements like these and create a system that has additional attributes and applications over existing research works.

Chapter 3

System Overview

This chapter provides a top-level overview of the functionality and building blocks of the system. This is depicted in Figure 3.1.

As with any VLC system, there is a need to integrate the data transfer functionality with the intended lighting functionality. In practice, this main lighting functionality should be the only perceptible component of the system, with the data transfer being imperceptible. This is achieved by transmitting the data in the form of high-frequency oscillations such that they are not noticeable to the human eye. Secondly, the transmission of data should not degrade the primary lighting feature itself. The algorithms used to accomplish this are described in the subsequent chapters, but first, we shall outline the functional blocks in the system and their interaction.

With the goal of designing an LED display that can also be used for sending and receiving data, the system can be visualized as a fusion of a typical communication system with an LED Display. For the purpose of this project, a prototype consisting of a 4x4 matrix of RGB LEDs is built. Thus, the display driver is a fundamental block for LED interfacing. It is also essential to devise an addressing scheme so that the driver is able to change the colours of individual pixels. The addressing can be as simple as assigning microcontroller pins to each LED, as well as something more complex such as select-lines for rows and columns. In the case of RGB LEDs, the pixel colour is defined by the brightness of the red, green, and blue channels. The driver can modulate the brightness by using varying currents or by varying the duty cycle of a PWM signal.

For the communication aspect, blocks such as sampling, signal conditioning, encoding, and decoding are included in the design. Since the pixels themselves are used for performing data transmission also, the encoded data is provided to the display driver along with the content to be displayed on the screen. Encoding ensures that the bits are represented in the form of pixel colours. Similar to the case of changing colours of the pixels, an addressing scheme is also necessary to sense the light incident on individual LEDs. With the inherent sensitivity of the LEDs towards incident light being low, appropriate signal conditioning is employed to amplify the received signal. This is followed by a sampling unit, and finally by a decoder, so as to extract accurate data from the sampled values.

It must be noted that this is a generic design based on the system's functionality. In practice, some of the blocks may be unnecessary, while some may

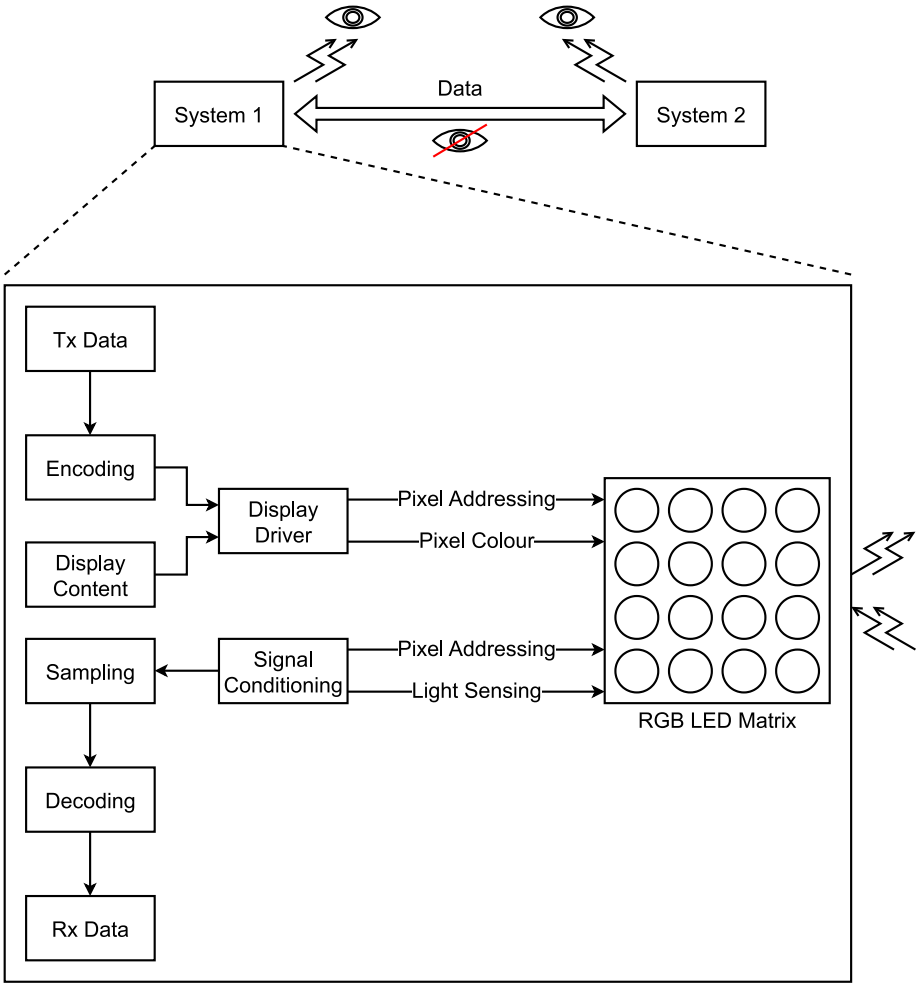

Figure 3.1: **System Overview**

even need additional complexity and optimization. Furthermore, it could be necessary to implement supplementary interaction between these blocks. The design of some blocks also offers scope for customization since it is possible to implement these in hardware as well as software. This is decided based on the specific needs of the system. These attributes will be discussed in chapter 4 and chapter 5.

Chapter 4

Hardware Design

In this section, I will describe the design of the hardware components in the system.

4.1 Selection of RGB LED and Communication Colour

Efficient data transfer requires the use of LEDs with a clear lens and low viewing angles. This choice of LEDs ensures that the emitted light is focused in a specific direction, optimizing the transmission of data signals. To identify the most suitable LEDs for the data transfer application, a series of tests were conducted using the devices listed in Table 4.1.

Once the LED devices were evaluated, the next step was to determine the best colour combination for communication purposes. In this regard, the performance of red, green, and blue LEDs was specifically examined. The evaluation focused on their ability to function both as transmitters and receivers in the data transfer system. By assessing the performance of red, green, and blue LEDs, the most effective colour combinations for optimal data transmission were identified. This initial experimentation was performed using a simple setup shown in Figure 4.1.

Figure 4.2 shows the five best responses among the several colour combinations of different LEDs. Based on this, LED 3 (Kingbright WP154A4SEJ3VBDZGC-CA) was found to work best as a photo sensor, and hence, best suited for com-

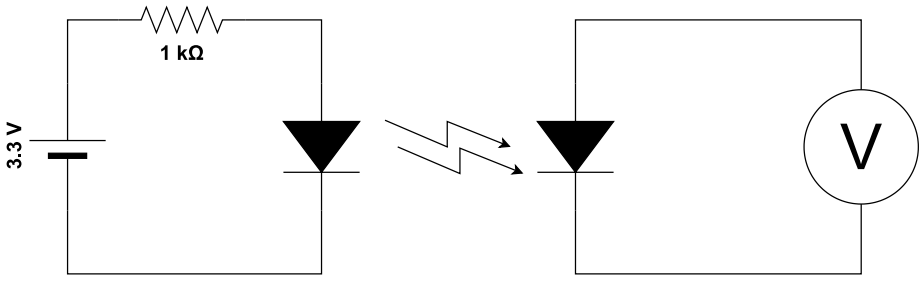

Figure 4.1: **Basic setup for initial experimentation**

Table 4.1: **List of LED devices under consideration for use in this project**

	Manufacturer	Model	Viewing Angle
LED 1	Inolux	HV-5RGB25	25°
LED 2	Kingbright	WP154A4SUREQBFZGC	60°
LED 3	Kingbright	WP154A4SEJ3VBDZGC-CA	50°
LED 4	Bivar	R50RGB-4-0045	45°

munication purposes. The results of some of the colour combinations for the chosen LED are displayed in Figure 4.3. It can be seen that the incidence of red light on red LED gives the best response followed by green light on red LED (similar to the observations in [17]).

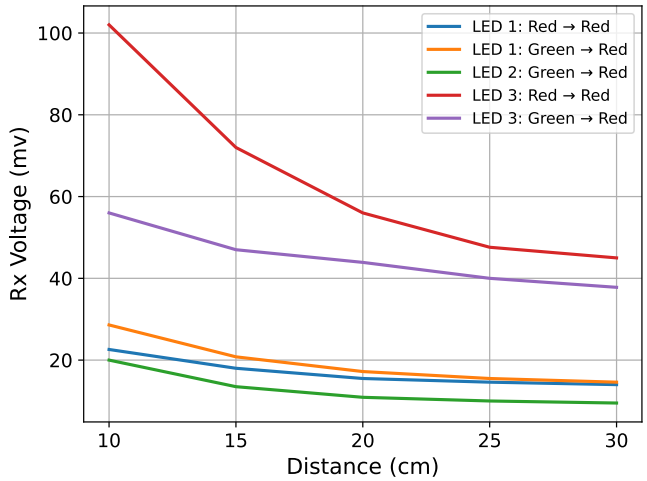

Figure 4.2: **Best Tx → Rx responses among various colour combinations of different LEDs**
LED 3 (Kingbright WP154A4SEJ3VBDZGC-CA) is most suited to be used as a sensor

Subsequently, the mutual interference of red and green light was studied. For this purpose, a red and a green LED were used as transmitters and another red LED is used as a sensor. It can be seen in Figure 4.4 that there is considerable interference between when red and green signals when they are simultaneously incident on a red LED acting as a sensor. Due to this, for the rest of this thesis, only the red-to-red combination is used for data transfer, since it is more efficient than its green-to-red counterpart. Even though green light is not used for transmitting data, a pixel displaying some green component can hamper the red-to-red communication, specifically when the green source is located close to the red sensor. This is especially true in an RGB LED, which has the red and green components packaged in a single device. Light emission from the green component could potentially affect the sensing abilities of the red component.

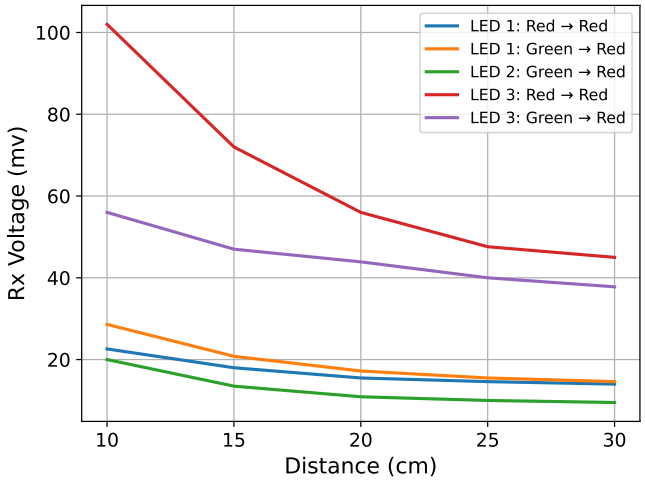

Figure 4.3: **Results of testing different Tx → Rx combinations with LED 3 (Kingbright WP154A4SEJ3VBDZGC-CA)**
Red → Red communication is most effective

To test this, a red emitter and red sensor were used. The tests were repeated after switching on the green component of the device which houses the red sensor. As seen in the results (Figure 4.5), the effect of switching on the green component is negligible and it does not affect the red-to-red communication.

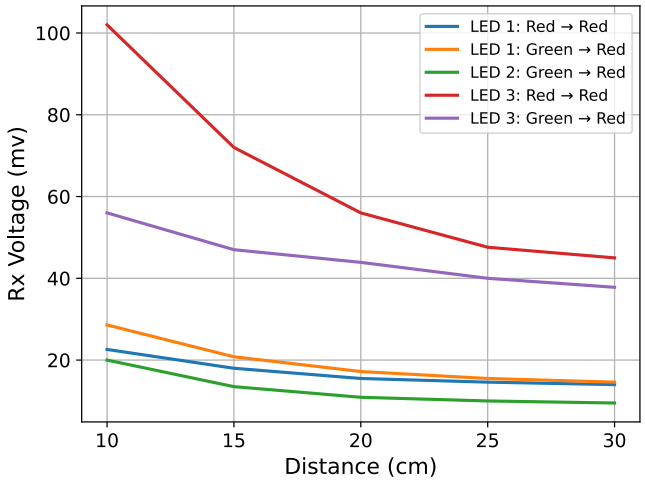

Figure 4.4: **Mutual interference between red and green light during simultaneous incidence on the red sensor is significant**

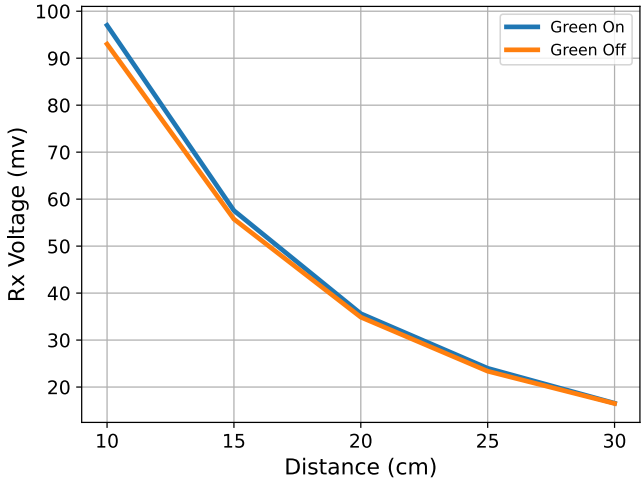

Figure 4.5: **Green emitter does not significantly affect a red sensor situated in the same RGB LED device**

4.2 Circuit Design

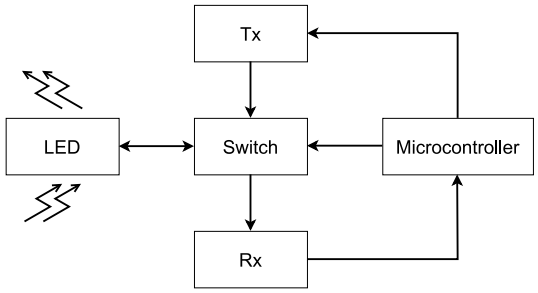

Figure 4.6: **Hardware blocks necessary for system operation**

At a high level, the system functionality requires certain key blocks in the circuit. These are depicted in Figure 4.6 and explained below:

1. **Transmitter (Tx) Block**: This block comprises the circuitry necessary for operating the LED in its normal forward bias mode when it functions as a transmitter or display.

2. **Receiver (Rx) Block**: The Rx block consists of biasing and conditioning components that prepare the LED to function as a photosensor. This block is responsible for converting the received optical signals into electrical signals that can be further processed and decoded.

3. **Switching Components**: Switching components play a crucial role in the circuit as they facilitate the seamless transition of the LED between its roles as a transmitter and a receiver. These components enable the

circuit to switch between the Tx and Rx modes, ensuring that the LED is correctly biased and operated based on the intended function at a given time.

4. **Microcontroller**: The circuit needs a control unit for coordinating and managing the operation of the various blocks. It provides the necessary intelligence to control the LEDs, switching components, and decode the received signals.

These blocks work together synergically to enable the integration of data transfer capabilities in the LED display.

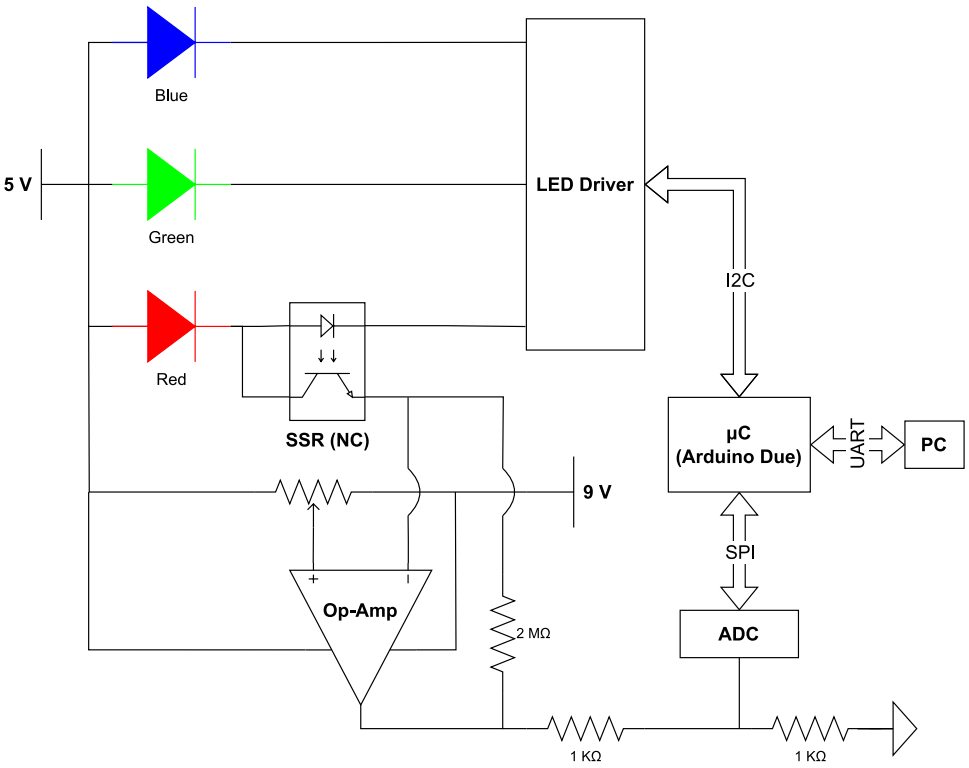

Figure 4.7: **Circuit design illustrating the interface between the various components**

The display and Tx functionalities can be implemented using the onboard PWM pins of the microcontroller. However, this is not feasible when the system is scaled to incorporate a large number of LEDs. Hence, it is beneficial to employ a PWM driver IC that can interface multiple LEDs and communicate with the microcontroller via a serial communication bus. In this project, the *PCA 9956BTW* LED Driver designed by NXP Semiconductors is used. It supports up to 24 LED channels and offers benefits such as dual control (current and duty cycle) for LED brightness [18], which have been exploited later in this project.

In order to enable accurate detection of incoming light signals, the Rx block should ensure proper reverse biasing and signal amplification. As mentioned in section 4.1, only the red component is used for reception, and when the

red component is sensing, the blue and green components could potentially be displaying pixel data. This puts forward the need to be able to operate one component in reverse bias while the other two operate in forward bias. This does not pose a challenge when the three components are independent of one other, however, the LED device in use is a 4 terminal device with a common anode and 3 separate cathodes for each of the three components. As a solution to this challenge, this project presents a design with three voltage levels namely 0V (GND), 5V, and 9V. The common anode is continuously maintained at 5V and the anode is switched between 0V and 9V to operate the LED in forward- and reverse- bias respectively. In addition to the reverse bias, it is imperative to amplify the received signal. A *MCP619*-based transimpedance amplifier is used for this purpose. Finally, this amplified signal is converted to the digital form. Similar to the PWM case, to ensure scalability, a dedicated Analog to Digital Converter (ADC) is used instead of the microcontroller's built-in ADCs. The Microchip MCP3008 offers 8 independent ADC channels that can communicate with the microcontroller via Serial Peripheral Interface (SPI).

For the switching operation, the components should enable seamless mode switching between the Tx and Rx blocks. Due to biasing requirements, sensing and emission of light cannot be performed by the same LED simultaneously. In other words, the LED can sense light only during the off-time of its PWM cycle. By leveraging this property, the circuit can be made more efficient. Rather than using a separate control signal to switch between the Tx and Rx blocks, the PWM signal itself can be used to connect and disconnect the Rx block to the LED. The *IXYS CPC1125N* solid-state relay fits these requirements perfectly. For the processing unit, the *Atmel SAM3X8E*-based Arduino due board is used. The system interface between an RGB LED and other Rx, Tx, and switching components is shown in Figure 4.7. The circuit schematics for one row of LEDs are included in Appendix A.

4.3 Implementation

As a prototype for this thesis, two 4x4 LED matrix displays are developed. Apart from the microcontroller, the other hardware components are implemented on a Printed Circuit Board (PCB) to achieve compactness and space effi-

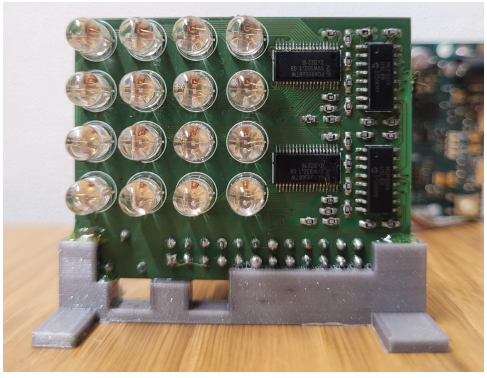

Figure 4.8: **Front view of the PCB implementation of the system**

Table 4.2: **List of the major hardware components used in this system**

Component type	Manufacturer	Model	Qty
RGB LED	Kingbright	WP154A4SEJ3VBDZGC-CA	16
SSR	IXYS	CPC1125N-CA	16
LED Driver	NXP	PCA9956BTW	2
Op-Amp	Microchip	MCP619	4
ADC	Microchip	MCP3008	2

ciency. Additionally, using a PCB ensures the repeatability of experiments and consistent results. The layout and connections on the PCB are designed to be reproducible, allowing for consistent performance across multiple prototypes. This helps eliminate variations that may arise from using different wiring methods or manually assembled circuits. The PCB also provides structural support and protection for the components, reducing the risk of damage or accidental disconnection. The soldered connections on the PCB offer more reliability and stability compared to loose wires or point-to-point wiring. Table 4.2 shows the main hardware components used in one matrix display. Figure 4.8 shows the front view of the PCB, with the components soldered onto it. The PCB designs can be referred to in Appendix B.

Chapter 5

Software Design

5.1 Skeletal Components

With regards to the data communication requirements and the specified hardware design, a couple of software components form the heart of the software system.

1. **Timer Interrupts**

   As with any communication system, ensuring accurate timing is key to effective data transfer. Moreover, in a multi-modal system, timing control is important to facilitate fairness between the various modes of operation. Timers and interrupts help enhance the reliability and performance, and responsiveness of data communication systems. They allow protocol-specific timing requirements to be enforced and enable task switching at regular intervals. By implementing handlers for the timers, the microcontroller can be configured to perform certain tasks at every tick of the timer. When timers are used for controlling communication, the signal level can be changed at every tick. Thus, the tick frequency essentially decides the data rate of the system.

2. **Peripheral Interfacing**

   The hardware employs two types of peripherals, namely LED Drivers and ADCs. These can be interfaced via I^2C and SPI respectively. Although open-source libraries are available for the given LED driver and ADC, using them is not the preferred approach. They come with unnecessary abstraction layers that can impact performance. Abstraction is not crucial in this project since a static microcontroller platform is being used. Therefore, this project focuses on developing custom libraries that prioritize fast performance and meet their specific requirements. With such a custom design, the software can be tailored to the unique needs of the system and performance can be optimized for efficient execution. This allows for more control over the software and ensures that it aligns perfectly with the objectives.

5.2 Practical Limitations

To design efficient software for data communication, it is crucial to have a thorough understanding of the system's sampling, signal reconstruction, and processing abilities. This is essential to determine the sampling rate at which the LEDs can reliably capture and detect changes in the transmitted signal. Secondly, the reconstructed signal needs to be reliable and consistent to accurately represent the transmitted information. By evaluating the signal reconstruction capabilities of the system, it becomes possible to assess the accuracy and fidelity of the received data.

In order to gather this knowledge, experiments were conducted by using the transmission of a square wave between two LEDs as a test scenario. This allows for the evaluation of the system's ability to accurately transmit and receive digital signals. By measuring the fidelity of the received square wave, the software design can be fine-tuned to ensure robust and efficient data communication.

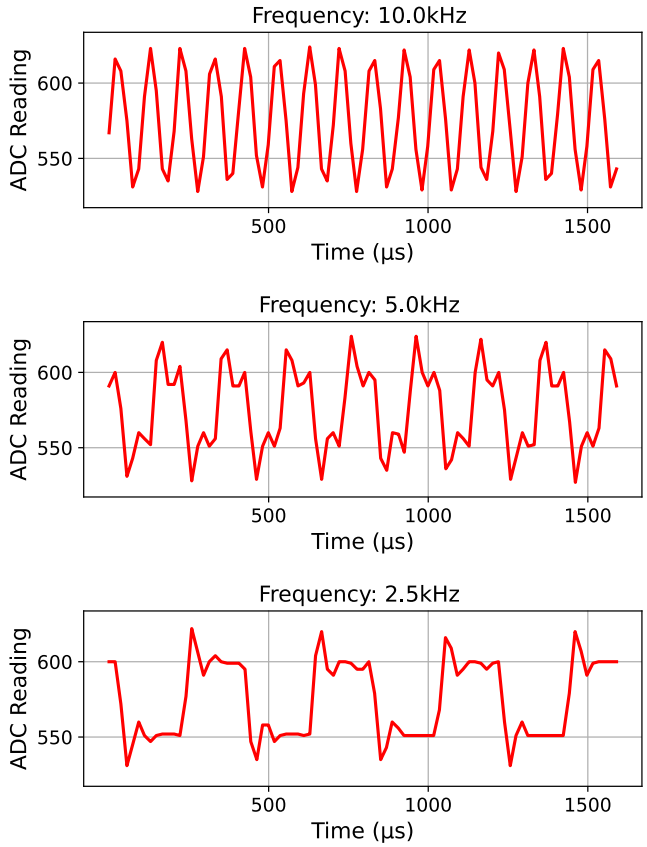

Figure 5.1: **Sampling results for square waves of different frequencies**

Figure 5.1 shows the results of these experiments. As the frequency of the wave on the transmitter side is increased, the "square"-nature of the reconstructed signal reduces. This can be attributed to the settling time of the sensor. When the incident light exhibits a level change, the sensor output undergoes

some oscillations and overshoots before settling at the new value. This is evident in the $2.5Khz$ case. However, for higher frequencies, the level of the transmitted signal changes faster than the settling time of the receiver. The average settling time for the receiver was measured to be $200\mu s$, for rising as well as falling edges. However, the half-point of the level change in much lesser time. The half-time was measured to be $25\mu s$. Thus, by using the half-point as a threshold, the signal then be efficiently reconstructed even at higher frequencies, without requiring the sensor to settle to the level change.

Another critical factor in the sensing of light signals is the presence of ambient light. It leads to an additional component of light, apart from the data signal, being incident on the sensor. Thus, a change in lighting conditions can change the square wave levels read by the ADC. This also changes the aforementioned threshold. This effect was mitigated by sampling the ambient light intensity at the start. This value is then subtracted from all subsequent samples, to yield a "relative" incident intensity. Here, it was assumed that the ambient light acts as a constant component, shifting the *HIGH* and *LOW* levels of the pulse equally. The second assumption is that the ambient lighting conditions remain constant throughout the duration of the data transfer.

Next, a series of experiments were conducted to profile the software functions. It was observed that I^2C and SPI transactions are the most critical operations. The results of the profiling are displayed in Table 5.1.

Table 5.1: **Profiling results of software bottlenecks**

Function	Type of Operation	Average time
Changing LED State	I^2C Transaction	$40\mu s$
Reading ADC	SPI Transaction	$20\mu s$

With these results, it becomes possible to design an efficient software solution that maximizes the data transfer rate, minimizes errors, and optimizes the overall performance of the LED-based communication system.

5.3 Receiver Functionality

As discussed earlier, the sensing can only be carried out during the inactive periods of the display cycle. However, there is a challenge regarding the synchronization between the display's PWM cycle and the microcontroller's ability to process the received signal. The LED driver, which controls the display PWM cycle, does not provide information to the microcontroller about the inactive phase of the cycle. But the microcontroller requires control over the off-time of the duty cycle in order to effectively process the received signal.

To overcome this limitation, a solution is implemented where the microcontroller takes control of managing the display cycle instead of relying on the LED driver. This is achieved by the microcontroller by instructing the LED Driver to turn the LED on or off at every rising or falling edge of the PWM cycle, respectively.

By taking charge of the display cycle management, the microcontroller can synchronize its operations with the display's PWM cycle and effectively perform the necessary sensing tasks during the inactive phase. But there still exists a

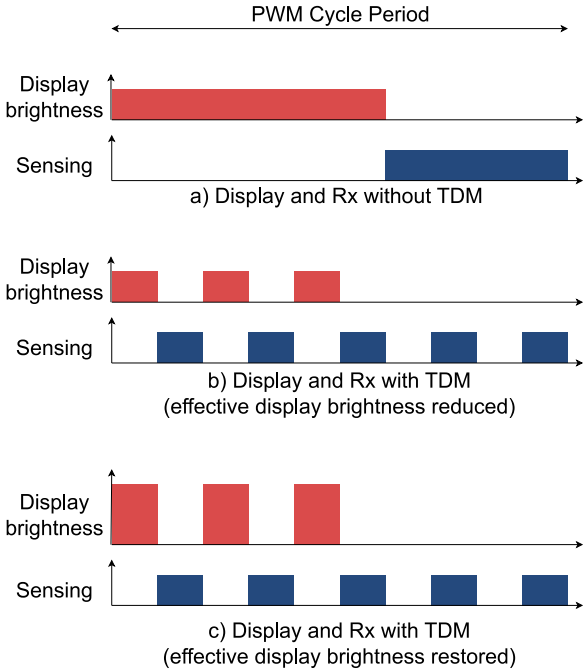

Figure 5.2: **Integrated display and Rx functionality using TDM**

major challenge resulting from an irregular sensing interval that relies on the duty cycle. To address this challenge, a potential solution is to implement a Time-Division Multiplexing (TDM) approach, where the display and receiver functions operate alternately within equal time slots. However, this approach comes with a trade-off: the duty cycle of the display is reduced by half.

To mitigate the impact of this reduced duty cycle, the system takes advantage of the LED Driver's dual-control property. By doubling the current, the reduction in the duty cycle can be compensated. This enables the display to maintain its brightness and visual performance while accommodating the necessary sensing operations during inactive periods. This procedure is demonstrated in Figure 5.2.

5.4 Transmitter Functionality

For integrating the transmission functionality with the functions, a common approach is to employ TDM similar to what is used for the receiver. However, in this scenario, there is an inherent challenge: transmitting data during the display cycle can impact the displayed pixel colour, resulting in an undesired visual effect.

To address this issue, a solution is to embed the data transmission within the displayed intensity itself. This means that the transmission of data should generate the desired LED intensity, without affecting the pixel colour. The key requirement for such a system is that the LED should maintain the desired intensity regardless of the data bits being transmitted. In other words, the symbols representing '0' and '1' should produce the same effective intensity.

One effective coding scheme that achieves this objective is Manchester coding. By utilizing Manchester coding, the system ensures that a constant intensity is maintained throughout the transmission process [28]. However, due to the *OFF*-intervals of the Manchester symbols, the overall intensity is reduced by half. To counteract this reduction in intensity, a current compensation technique can be applied to restore the effective intensity to the required value.

In this project, the *IEEE 802.3* convention for the Manchester symbols is used. By employing Manchester coding, the system can achieve consistent LED intensity regardless of the transmitted data, thereby preventing unwanted visual artifacts. Furthermore, by applying the current compensation technique, the system ensures that the overall effective intensity meets the desired specifications. As shown in Figure 5.3, by combining Manchester coding with current compensation, the system can successfully perform reliable data transmission without compromising the quality of the displayed content. With this method, the data rate is fundamentally limited by the intensity of the pixel. Techniques aimed at improving this data rate are explored in chapter 6 and chapter 7.

Although Manchester coding fits the requirements of the transmitter display, it is also essential for the receiver to able to detect and identify Manchester signals. As mentioned in section 5.3, the sampling operation of the receiver is limited to half of the duty cycle. Thus, it is not possible to sample the entire Manchester symbol. But that does not pose a problem, because the symbol can be reconstructed even when one of its halves is known. Thus, the receiver samples only the second half of the transmitted symbol, and decodes it to obtain the correct bit value.

Since the pixel intensity values range from 0 to 255, both inclusive, the time period is divided into 255 slots. The number of slots transmitting Manchester code is determined by the pixel intensity. The rest of the slots in the period remain inactive.

5.5 Message Structure

The message structure in this system follows a specific format to ensure reliable and accurate data transmission. The components of the message are outlined below:

1. **Preamble**

   The message begins with a preamble, which serves as an initial synchronization sequence to establish communication between the transmitter and the receiver. A series of 40 *HIGH* bits are sent as a preamble, thus aiding in aligning the timing and allowing the receiver to identify the start of a message.

2. **Target**

   The preamble is followed by a set of 255 slots which contains some initial *HIGH* bits followed by the rest inactive slots. The number of *HIGH* bits is decided by the desired pixel intensity. This number is defined as the "target". From section 5.4 it is known that the receiver only samples the second half of the Manchester symbols. Hence, the receiver is unable to distinguish between an inactive slot, and a slot transmitting a '0'-bit. The

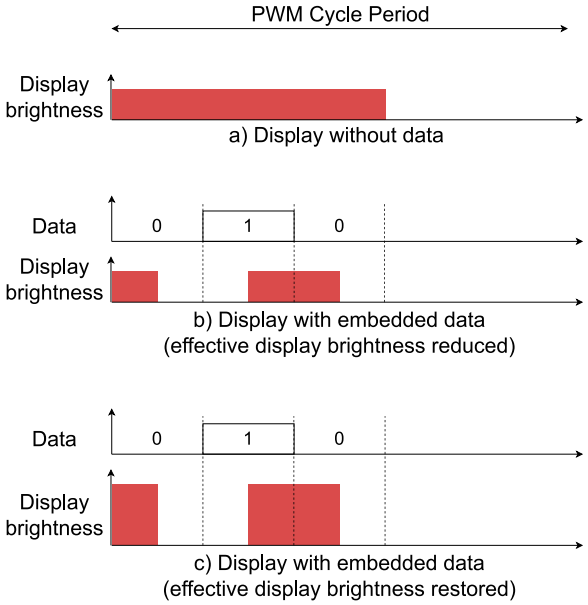

Figure 5.3: **Embedded display and Tx functionality using Manchester coding**

purpose of this target bit-set is to inform the receiver about the number of active slots in the following sets of 255 slots each. It should be noted that in the message structure, the number of bits refers to the actual number of bits in the transmitted data which may not necessarily equate to the number of slots.

3. **Data Length**

   Following the target, the message structure includes four bytes that indicate the total number of bytes contained within the message. This information is crucial for the receiver to determine the length of the message and correctly process the incoming data.

4. **Data Chunks**

   The actual data within the message is divided into chunks of 64 bytes each. These chunks enable efficient handling and processing of the data, as breaking it down into manageable segments enhances the system's overall performance.

5. **CRC-8**

   Each 64-byte chunk is then accompanied by a CRC-8 (Cyclic Redundancy Check) code. The CRC-8 is a form of error detection code that ensures data integrity during transmission. By performing a mathematical calculation on each byte within the chunk, the CRC-8 generates a checksum that can be used to verify the accuracy of the received data. The receiver can compare the calculated CRC-8 value with the transmitted value to detect any errors that might have occurred during transmission.

Overall, this structured message format, consisting of a preamble, length indicator bytes, data chunks, and CRC-8 codes, is designed to enable reliable and robust data transmission. By including synchronization, length information, data segmentation, and error detection, the system can effectively transmit and validate data, ensuring the integrity and accuracy of the received information.

Chapter 6

Colour Augmentation

As mentioned in chapter 5, the data rate in this system is limited by the intensity of the displayed pixel. When the pixel intensity is zero, no data can be transmitted. To overcome this limitation, it becomes necessary to increase the pixel intensity in a way that the modified colour is not noticeably different from the original colour. This technique can also be applied to non-zero intensity values to further increase the data rate.

To achieve this, the focus is primarily on maximizing the red component of the pixel while keeping the green and blue components unchanged. The objective is to ensure that the visual difference between the colours is below the Just Noticeable Difference (JND) threshold of the human eye. In order to accomplish this, it is essential to study the visual response to the displayed colours.

6.1 Colour Space

The RGB colour space, commonly used for digital representation, does not provide information about human perceptibility and is not perceptually uniform. This means that equal Euclidean distances in the RGB space do not correspond to the same perceived colour difference by humans. To accurately measure the perceived difference between two colours, a perceptually uniform colour space needs to be employed.

In this particular case, the CIELAB colour space is utilized. The CIELAB colour space offers perceptual uniformity, where the Euclidean difference in this space directly corresponds to the Delta-E metric. Delta-E is a measure of the perceived colour difference, where a value of 1 Delta-E represents a Just Noticeable Difference (JND) between two colours. Table 6.1 shows the comparison of using RGB and CIELAB colour spaces to find the colour difference.

By leveraging the CIELAB colour space, it becomes possible to quantitatively measure and evaluate the perceived colour differences between the original colour and the modified colour with increased red intensity.

Table 6.1: **CIELAB colour space gives a better measure of perceived colour difference than the RGB colour space**

Colour	RGB		CIELAB	
	Coordinates	Difference	Coordinates	Difference
	5, 255, 255	29	91.13, -47.99, -14.10	0.96
	34, 255, 255		91.27, -47.07, -13.88	
	226, 255, 255	29	97.99, -9.32, -3.17	10.05
	255, 255, 255		100, -2.45, 0	

6.2 R_{max} Algorithm

The processor and the LEDs operate in the RGB space. Thus, conversions between the RGB and CIELAB spaces are necessary to find the maximum permissible intensity of the red component, defined as R_{max}. The algorithm for this process can be formulated as follows:

Algorithm 1: Computation of R_{max} for a given colour from the RGB space

Input : $0 \leq R_0 \leq 255; 0 \leq G_0 \leq 255; 0 \leq B_0 \leq 255$
Output: $R_0 \leq R_{max} \leq 255$
$l_0, a_0, b_0 \leftarrow$ `Convert-To-LAB(`R_0, G_0, B_0`)`
for $R_0 \leftarrow R_1$ **to** 255 **do**
  $l_1, a_1, b_1 \leftarrow$ `Convert-To-LAB(`R_1, G_0, B_0`)`
  $\Delta E \leftarrow$ `sqrt(`$(l_1 - l_0)^2 + (a_1 - a_0)^2 + (b_1 - b_0)^2$`)`
  if $\Delta E > 1$ **then**
    $R_{max} \leftarrow R_1$
    break
  end
end

6.3 Implementation

The most rudimentary approach is to implement the algorithm from the previous section on the microcontroller and perform the computation in real-time. However, the conversion from RGB to CIELAB colour spaces is computationally expensive and cannot fulfil the real-time demands of the system. Another approach is to compute the R_{max} values for each colour in the RGB space and write the data to the microcontroller's EEPROM. However, R_{max} is a 1-byte value, and with 256^3 possible colours in the spectrum, the storage size for such a dataset is 16MiB, while the Arduino Due has an EEPROM of only 512 bytes. Thus, the next step is to develop a low-cost approximation function for computing R_{max} from the R, G and B values. This serves as a trade-off between execution speed and visual quality. For the approximate function to be formulated, the behaviour of R_{max} in the RGB space needs to be studied. The

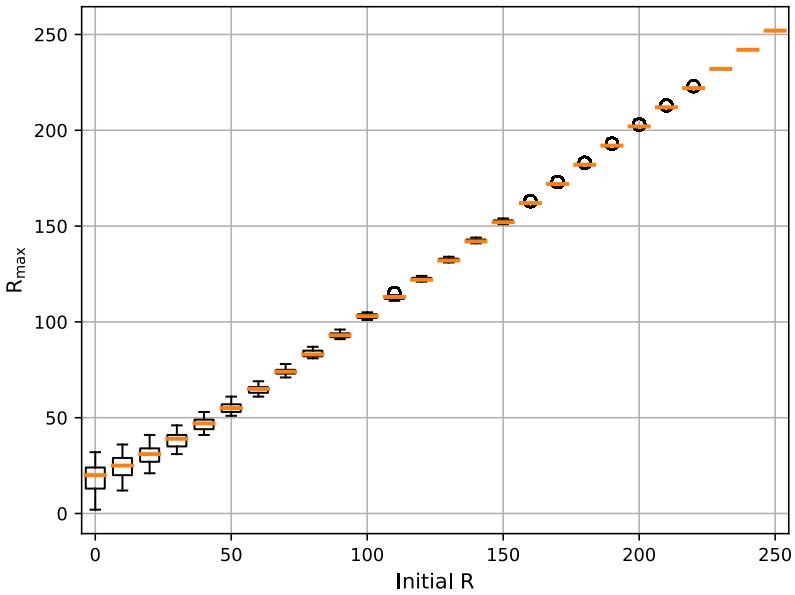

Figure 6.1: **Variation in R_{max} decreases as R increases**

distribution of R_max for various R values is shown in Figure 6.1.

The box plot gives an indication of the variation in R_{max} for a particular R. This variation is due to the dependence of R_{max} on G and B values as well. Thus, it is evident that for higher values of R, the dependence of R_{max} on G and B decreases. Hence, in this range, R_{max} can be estimated as a linear function of R alone. Analysis of the box plots yields two regions ($99 \leq R \leq 151$ and $152 \leq R \leq 255$) which are suitable for such an approximation. The estimation functions for these regions are derived to be $R_{max} = R + 1$ and $R_{max} = min(R + 2, 255)$ respectively Figure 6.3.

For $R < 99$, R_{max} needs to be approximated using G and B values as well. In order to maintain the cost-effectiveness of the operation, it is preferable to design linear functions rather than opting for higher-degree polynomials. Even though R_{max} varies non-uniformly, in a small section of the RGB space, it can be approximated by a linear function. By carefully studying the behaviour of R_{max}, these sections were identified. The process involves segregating the Blue-Green 2D space into 7 zones and deriving an estimation function for each zone. In some zones, a linear R_{max} vs R curve can be easily fitted. In the rest of the zones, R_{max} shows greater non-linearity and hence, further divisions are made on the red dimension. The approximation function can thus be formed as an amalgamation of multiple linear functions. The division of the Blue-Green space and the derived estimate functions are shown in Figure 6.4.

Finally, these parts are put together, to construct the procedure defined in algorithm 2.

Algorithm 2: Low-cost estimation of R_{max} for a given colour from the RGB space

if $R_0 \geq 152$ **then**
  $R_{max} \leftarrow min(R_0 + 2, \quad 255)$
else if $R_0 \geq 99$ **then**
  $R_{max} \leftarrow R_0 + 1$
else
  if $B_0, G_0 \in$ *Zone 1* **then**
    $R_{max} \leftarrow R_0 + 3$
  else if $B_0, G_0 \in$ *Zone 2* **then**
    $R_{max} \leftarrow \texttt{floor}(0.95 \times R_0) + 7)$
  else if $B_0, G_0 \in$ *Zone 3* **then**
    $R_{max} \leftarrow \texttt{floor}(0.89 \times R_0) + 13)$
  else if $B_0, G_0 \in$ *Zone 4* **then**
    if $R_0 < 20$ **then**
      $R_{max} \leftarrow \texttt{floor}(0.65 \times R_0) + 17)$
    else if $R_0 < 40$ **then**
      $R_{max} \leftarrow \texttt{floor}(0.75 \times R_0) + 15)$
    else
      $R_{max} \leftarrow \texttt{floor}(0.95 \times R_0) + 8)$
    end
  else if $B_0, G_0 \in$ *Zone 5* **then**
    if $R_0 < 20$ **then**
      $R_{max} \leftarrow \texttt{floor}(0.55 \times R_0) + 22)$
    else if $R_0 < 40$ **then**
      $R_{max} \leftarrow \texttt{floor}(0.75 \times R_0) + 18)$
    else
      $R_{max} \leftarrow \texttt{floor}(0.91 \times R_0 + 11.45))$
    end
  else if $B_0, G_0 \in$ *Zone 6* **then**
    if $R_0 < 20$ **then**
      $R_{max} \leftarrow \texttt{floor}(0.5 \times R_0) + 26)$
    else if $R_0 < 40$ **then**
      $R_{max} \leftarrow \texttt{floor}(0.7 \times R_0) + 22)$
    else
      $R_{max} \leftarrow \texttt{floor}(0.9 \times R_0) + 14)$
    end
  else if $B_0, G_0 \in$ *Zone 7* **then**
    if $R_0 < 20$ **then**
      $R_{max} \leftarrow \texttt{floor}(0.4 \times R_0) + 32)$
    else if $R_0 < 40$ **then**
      $R_{max} \leftarrow \texttt{floor}(0.6 \times R_0) + 28)$
    else
      $R_{max} \leftarrow \texttt{floor}(0.88 \times R_0) + 17)$
    end
  end
end

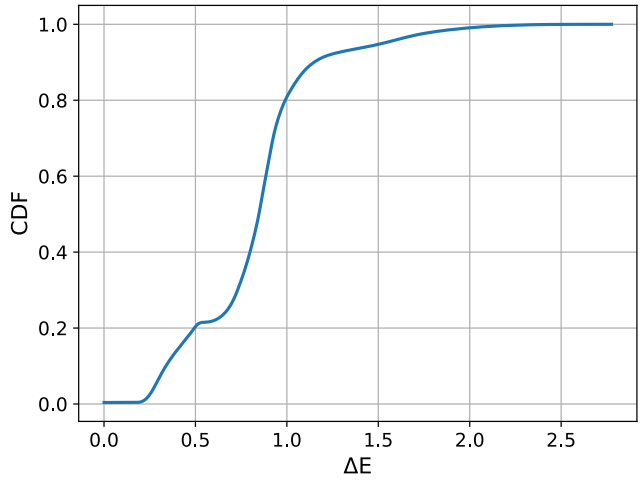

Figure 6.2: **CDF for ΔE values across the entire RGB colour space**

To analyse the impact of this approximation on the visual appearance, the ΔE metric between the modified and the initial colour was computed for every colour in the RGB space. The Cumulative Density Function (CDF) of all ΔE values indicates that for 80% of the colours in the spectrum, this colour modification yields a ΔE value of less than 1, and in over 90% of the cases $\Delta E < 1.2$.

It can thus be concluded that duty cycle maximization using with aforementioned estimation technique is an effective way to improve the throughput while maintaining the visual quality of the displayed pixel.

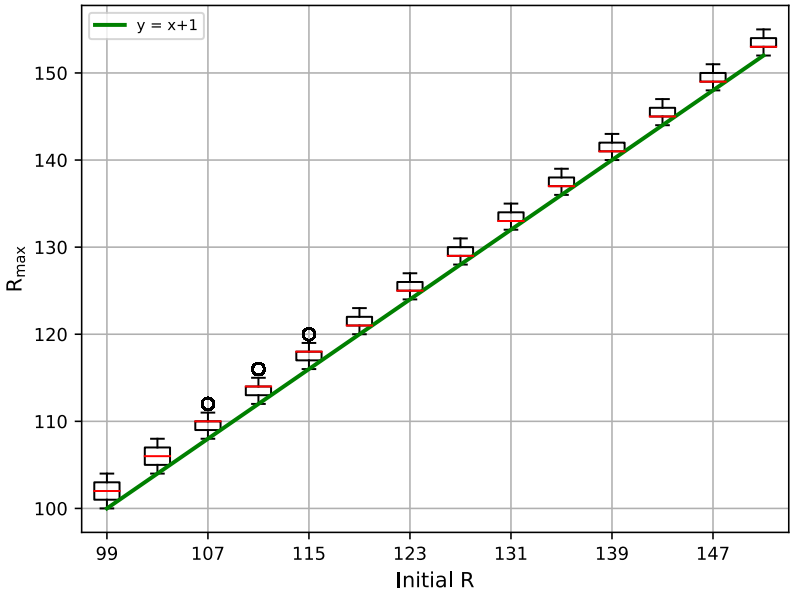

(a)

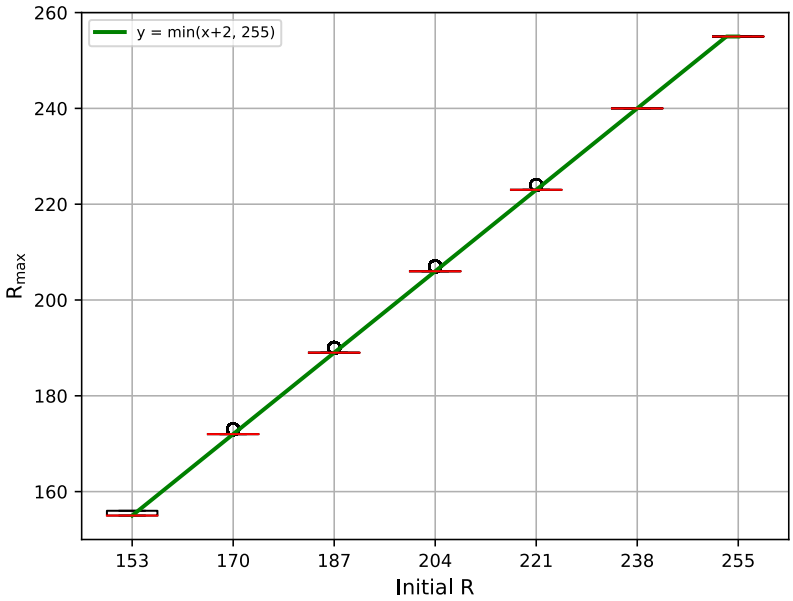

(b)

Figure 6.3: R_{max} **estimation functions for**
(a) $99 \leq R \leq 151$**, and**
(b) $152 \leq R \leq 255$

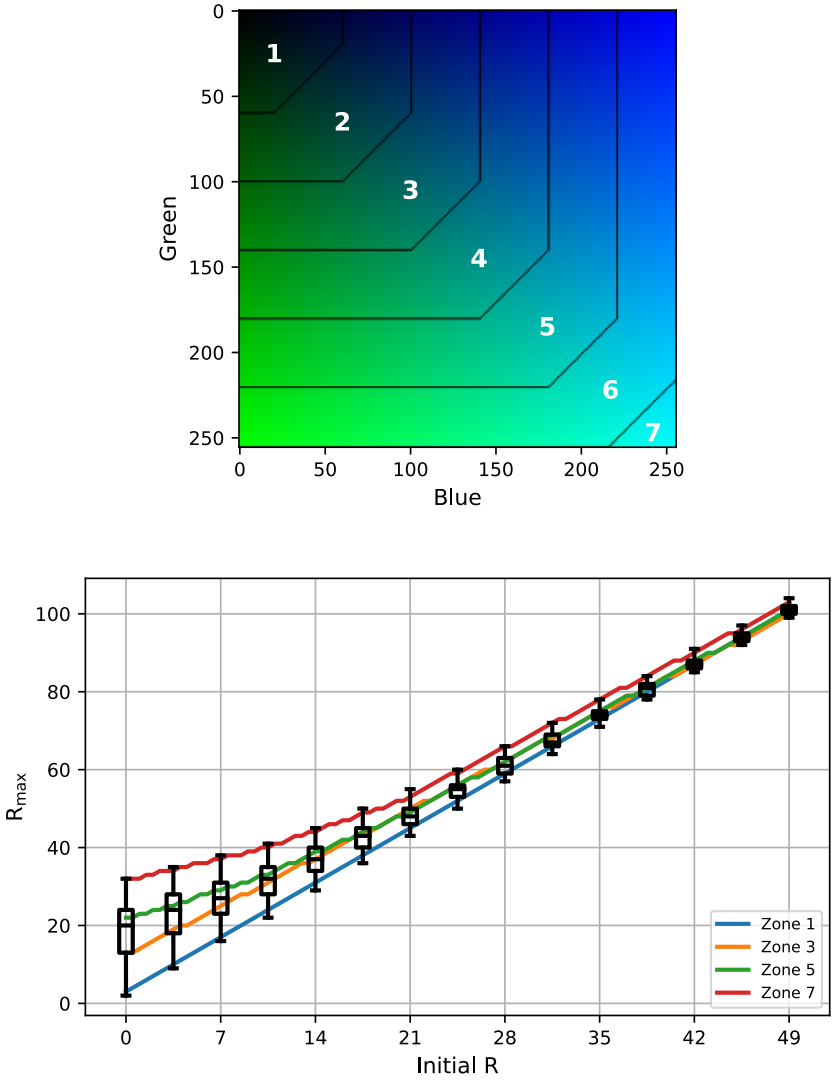

Figure 6.4: **Partitioning of the Blue-Green plane into 7 zones (top), and Estimation functions for $0 \leq R \leq 98$ in zones 1, 3, 5, 7 (bottom)**

Chapter 7

Many-to-One Communication

While scouting the possibilities of multi-channel communication, it was discovered that adjacent Rx-Tx channels cause mutual interference. Thus, adjacent LEDs cannot be used to operate two channels simultaneously. However, this points towards an interesting observation: mutual interference indicates that an Rx LED has the potential to receive data from multiple Tx LEDs and not just from the one positioned directly opposite it. This thesis proposes to exploit this property to maximize the utilization of the duty cycle and thus, enhance the data rate.

This is particularly useful when the Tx pixel colour has a low red component intensity. It is already known that the intensity of the red components controls the data rate of communication. Even with intensity maximization mentioned in chapter 6, the duty cycle is not always used to its full capacity. The utilization can be increased by having multiple Tx LEDs transmit different parts of data. Since the receiver is able to receive data from all these transmitters, it remains oblivious to the presence of multiple Tx LEDs and cannot differentiate among them. Therefore, this feature can be integrated into the transmission module, without requiring any modifications to the receiver module.

7.1 Feasibility

Implementation of this system demands an understanding of the sensitivity of an Rx LED to multiple other Tx LEDs. The obvious assumption is that the Rx LED should be able to receive data from the exactly opposite Tx LED and the 4 surrounding LEDs closest to the exact opposite LED. However, experiments proved that this was not the case. It was observed that the orientation of the LED plays a key role in this aspect. In this system, with the semiconductors aligned horizontally, an Rx LED shows greater sensitivity towards Tx LEDs that are at the same vertical elevation. In other terms, an Rx LED is more likely to receive data from LEDs that are in the same row as the exact opposite Tx LED. To explore this further, a series of square-wave tests were conducted to determine potential Tx LED sets for a particular Rx LED. The results for two of the configurations are shown in Figure 7.1 (Configuration 1) and Figure 7.2

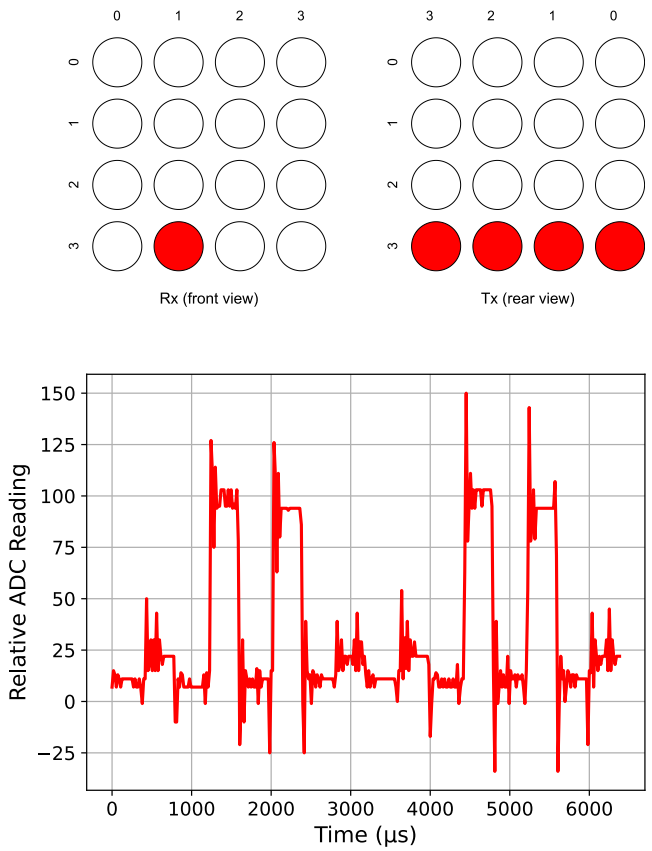

Figure 7.1: **Sampling results for a square wave transmitted in parts by multiple Tx LEDs (Active Tx and Rx LEDs are shown in red)**

(Configuration 2). In Configuration 1, two of the 4 peaks in a cycle have very low amplitudes. This implies that two of the Tx LEDs are not suitable to be used as potential transmitters for this particular Rx LED. However, with a similar Rx-Tx geometry, Configuration 2 produces different results. Although the amplitudes of the peaks are different, all are above a considerable threshold, this making them all four suitable as transmitters. This situation arises due to slight misalignment between the LEDs and displays, and geometric inaccuracies that exist in practice.

7.2 Initial Scanning Phase

From section 7.1, it is evident that for a particular Rx LED, the potential Tx set cannot be selected based on geometry alone. Moreover, small changes in the hardware alignment can cause the Rx LED to be less sensitive towards the selected Tx set. Thus, to ensure accurate data transmission, the system cannot rely on static Tx sets. Thus, we introduce a scanning phase that runs when the system starts. It involves each Rx LED attempting to sense light from each Tx

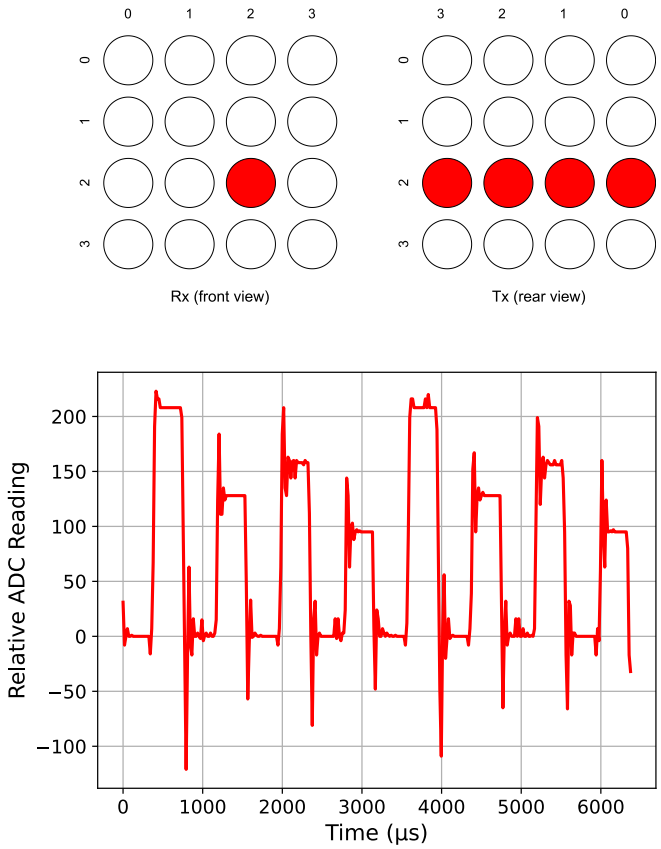

Figure 7.2: **Sampling results for a square wave transmitted in parts by multiple Tx LEDs (Active Tx and Rx LEDs are shown in red)**

LED. The Tx LEDs which are able to yield outputs above a certain threshold are selected as potential transmitters for the particular receiver.

7.3 Algorithm

With the feasibility aspect managed, maximum utilization of the duty cycle necessitates the development of an effective algorithm. For this purpose, the "target" of each Tx LED is taken into consideration. The target is defined by the desired intensity of the red component of the pixel (after the maximization from chapter 6 has been applied). The target is the number of slots for which the Tx LED remains active, in a 255 slot cycle. By using multiple Tx LEDs, the goal is to utilize as many remaining slots as possible. To avoid multiple LEDs transmitting at the same time and effectively wasting the available slots, we introduce a *token* system. Only the LED with the token is allowed to be active in a particular slot. Each cycle starts with the token being assigned to one of the LEDs. When it reaches its target, the token is passed to the next LED. This results in maximum utilization of the available 255 slots. This technique works

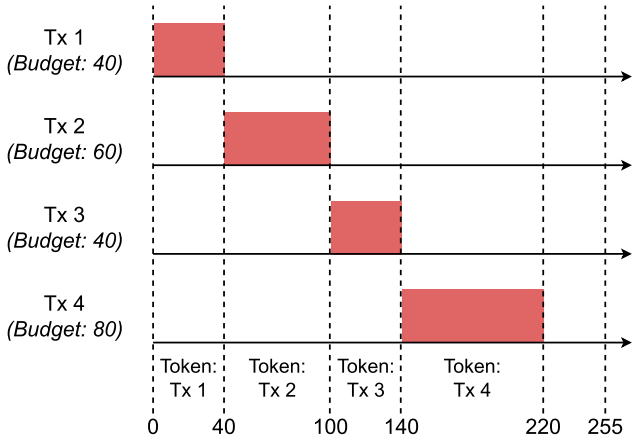

Figure 7.3: **Timing diagram for the use of multiple Tx LEDs when their total target is less than or equal to** 255

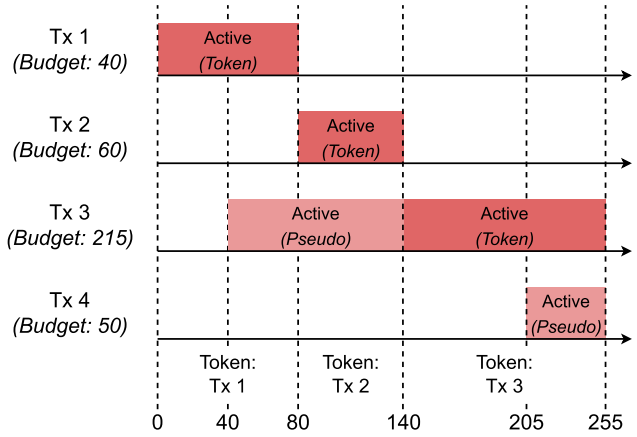

Figure 7.4: **Timing diagram for the use of multiple Tx LEDs when their total target is more than** 255

well when the total target is less than or equal to 255. The timing diagram for such a system is displayed in Figure 7.3.

However, when the total target exceeds 255, this procedure impacts visual quality, since some Tx LEDs are not able to achieve their target. In theory, when the total target is above 255, some of the slots should have multiple Tx LEDs active. This is also not a problem in practice because the Rx LED only considers the thresholded signal rather than the signal amplitude itself. With multiple Tx LEDs transmitting data, the *LOW* part of the symbol is not affected. For the *HIGH* part, the amplitude of transmission is higher than that in the single Tx LED case. With thresholding, this increased amplitude does not introduce any complications on the receiver side. This modification is carried out by extending the previously designed token system. We incorporate *pseudo-tokens* into the system, which are granted to Tx LEDs when the priority is to reach their targets. When the number of remaining slots in the cycle is

equal to the remaining target for a particular LED, it implies that it should be active in every subsequent slot, even when it does not have the token. Thus a pseudo-token is granted to LEDs that do not have the main token and have just enough slots left in the cycle to complete their target. The timing representation for this procedure can be seen in Figure 7.4. Adopting this approach augments the data rate of the system and causes no loss to the visual quality of the pixels.

Chapter 8

Evaluation

8.1 Setup

A pair of 4x4 RGB LED displays were used to evaluate the performance of the system under different conditions. The displays were placed facing each other, such that the LEDs were aligned, as shown in Figure 8.1. Although each display can operate as a transmitter as well as a receiver, for the purpose of the tests, Screen 1 was set as the receiver and Screen 2 as the transmitter. The Tx-Rx configuration from Figure 7.2 was used, with 4 transmitter LEDs and 1 receiver LED. Data transfer was performed using the red channel of both, the Tx LED as well as the Rx LED.

8.2 Parameters

This evaluation aims to assess the performance of the system based on two key parameters: Bit Error Rate (BER) and Throughput.

8.2.1 Bit Error Rate (BER)

The BER is a crucial metric that quantifies the accuracy of data transmission. It measures the ratio of incorrectly received bits to the total number of transmitted bits. A lower BER indicates a higher level of accuracy and reliability in the communication system.

8.2.2 Throughput

Throughput refers to the rate at which data can be successfully transmitted over the communication channel. It is measured in bits per second (bps) and directly impacts the system's data transfer capacity. As mentioned in section 5.1, the data rate of the system depends on the timer tick frequency. On the transmitter side, ticks control the transmission of Manchester code, and on the receiver side, the LED performs display and sensing at alternate ticks. Thus the maximum achievable bit rate (in bits per second) of the system is half the tick frequency (in Hz). However, the bit rate is different from the throughput, with the throughput being typically lesser than the bit rate. This is because throughput also accounts

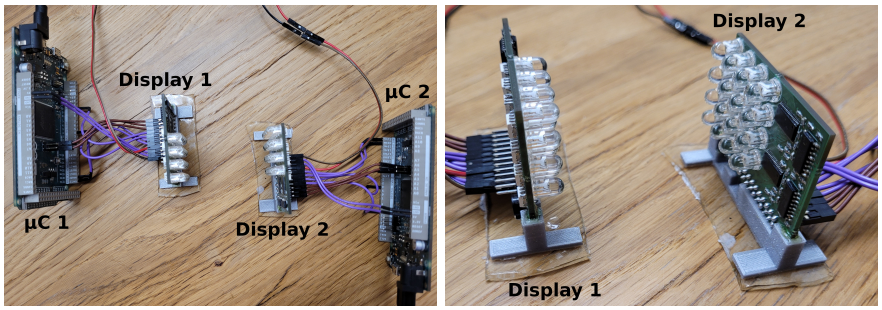

(a) (b)

Figure 8.1: **Evaluation Setup with two RGB LED Displays facing each other.**
(a) View of the full setup, including the microcontrollers
(b) Close-up view of only the displays

for all the additional time required for overheads, error-detection codes, and retransmission of erroneous chunks.

8.3 Evaluation Results

The evaluation takes into account the setting of several different variables, including the timer tick frequency, Tx target value, the distance between the transmitter and receiver LEDs, ambient lighting conditions, and the number of Tx LEDs involved. By analyzing these factors, we can gauge the effectiveness and reliability of the VLC system in various scenarios. Thus, several configurations consisting of various combinations of these variables were put to test. For each configuration, a data transfer of pseudo-random data of 20kB size was attempted. 10 iterations of each test were performed and the results from these were averaged, so as to investigate the effect of each parameter on the system performance.

8.3.1 Tick Frequency

In theory, higher tick frequencies are beneficial, since they allow for a greater amount of data to be transmitted within a given time frame. However, due to practical limitations, it is not usually feasible to send and receive data accurately when the frequency is increased beyond a certain threshold. It can be seen in Figure 8.2 that the BER was found to be below 0.01% for frequencies up to 9kHz. This indicates that the system has a very low error rate in this frequency range. However, a sharp rise in BER was observed above 9kHz frequency, suggesting a significant deterioration in data transfer. Since the BER had negligible dependence on the target value, it can be said that the bit errors are evenly distributed over the 255 slots.

Analysis of throughputs at different tick frequencies and target values is shown in Figure 8.3. As expected, initially, the throughput was observed to increase with an increase in tick frequency (Figure 8.3a). Also predictably, the throughputs increased nearly linearly with a linear increase in target value (Figure 8.3b).

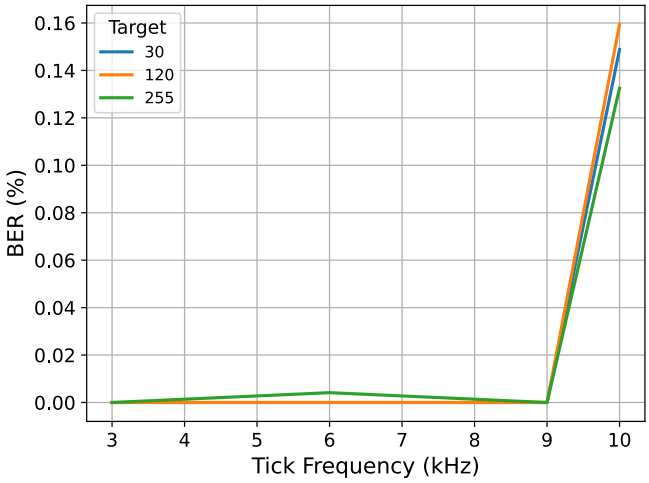

Figure 8.2: **BER is below** 0.01% **for tick frequencies up to 9kHz, and increases rapidly thereafter**

Interestingly, both the figures show that the throughput at 10kHz was lower than that at 9kHz, for all target values. This can be attributed to the increased number of errors at 10kHz, which outweigh the benefits of the increased frequency. As a consequence, the system's throughput is negatively affected. The presence of errors necessitates the retransmission of erroneous data chunks, which ultimately leads to a reduction in overall throughput. At 11kHz frequency, the communication was observed to become unreliable, resulting in a complete loss of throughput. This indicates that the system is unable to sustain reliable transmission and reception of data at this frequency.

8.3.2 Distance

While analysing the performance of the systems at various Rx-Tx distances, the strength of the received signal decreases with an increase in distance. Thus, a constant threshold between the *HIGH* and *LOW* signal values is not sufficient to correctly detect the signal state at different distances. Hence, before conducting the data transfer experiments at a particular distance, the threshold value was tuned, so as to achieve optimum performance.

The trends in BER vs Distance for various tick frequencies and target values are shown in Figure 8.4 and Figure 8.5 respectively. In Figure 8.4, the target value was kept constant at 255, across all frequencies. In Figure 8.5, a tick frequency of 9kHz was used, with varying target values. For a given frequency or target value, the BER was found to remain nearly constant, below 0.01%, for distances ranging from 5 to 20cm. This indicates a reliable communication performance within this distance range. However, at a distance of 40cm, the BER exceeded 20%, indicating a significant increase in transmission errors. It was also observed, that unlike the lower distances, at a 40cm distance, higher tick-frequencies result in a higher BER value, implying that the receiver is unable

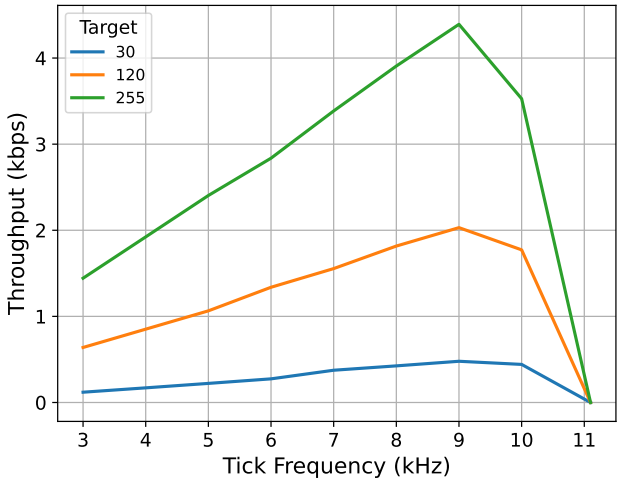

(a)

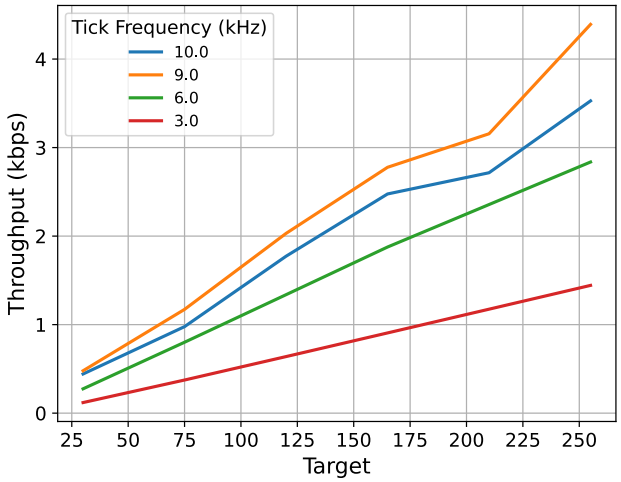

(b)

Figure 8.3: **Throughput curves showing:**
(a) a peak at a tick frequency of 9kHz
(b) a linear variation with the target value

to accurately decode a high-frequency digital signal sent from a larger distance. The results also showed that up to a distance of 20cm, the BER values are similar across varying frequencies and target values. Therefore, it can be stated at distances below 20cm, the communication quality is independent of the tick frequency (up to 9kHz) and the target value.

Similar to the observations from the previous subsection, the throughput was found to have decreased beyond the 20cm distance, due to the increase in BER.

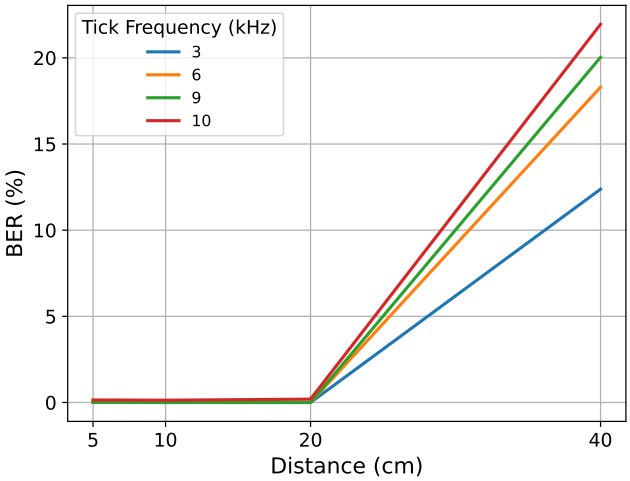

Figure 8.4: **BER increases beyond a 20cm distance, for all tick frequencies and a target value of** 255

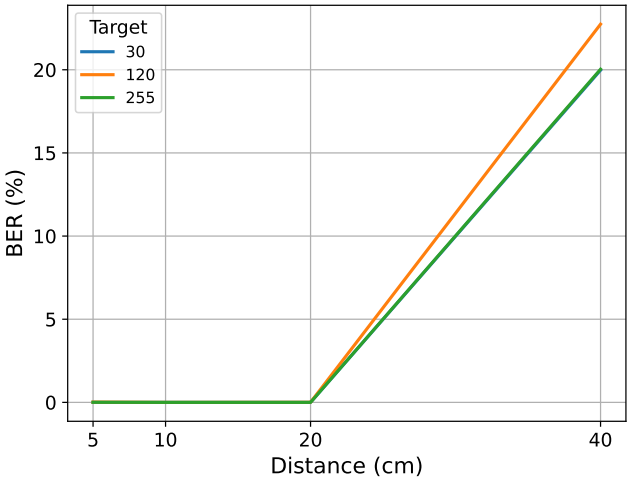

Figure 8.5: **BER increases beyond a 20cm distance, for all target values and a tick frequency of 9kHz**
(The curves for targets 30 ***and*** 255 ***nearly coincide)***

The results for different tick frequencies (Figure 8.6 and target values (Figure 8.7 were found to be consistent with the expectations.

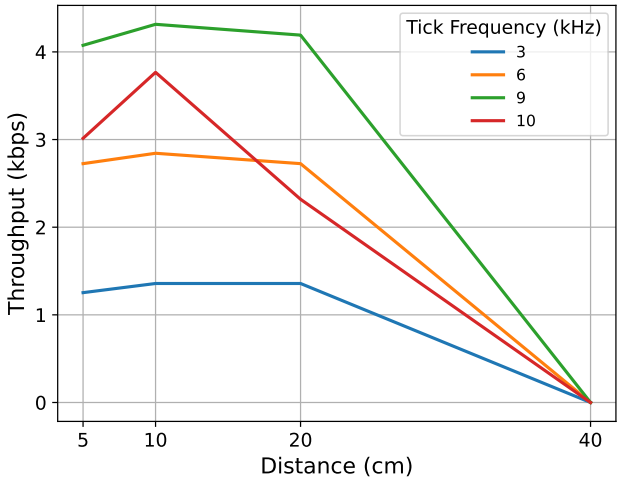

Figure 8.6: **Throughput decreases beyond a 20cm distance, for all tick frequencies and a target value of** 255

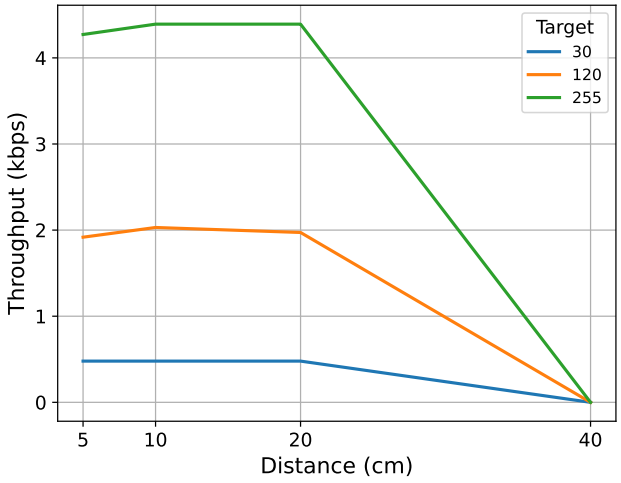

Figure 8.7: **Throughput decreases beyond a 20cm distance, for all target values and a tick frequency of 9kHz**

8.3.3 Ambient Lighting Conditions

Next, the performance of the system under various ambient lighting conditions is investigated. For this, three test scenarios with different lighting intensities were selected: dark (0 lux), indoor (300 lux), and outdoor (2600 lux).

The BER values were observed to remain constant under all ambient lighting conditions (Figure 8.8 and Figure 8.9). This suggests that the performance of the system is not significantly affected by changes in the lighting environment.

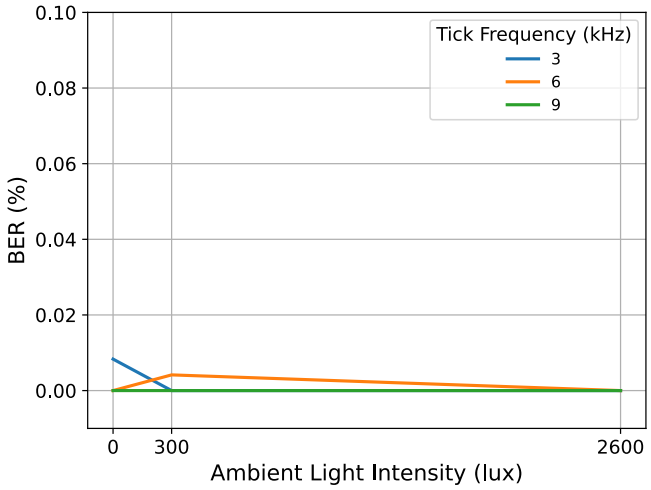

Figure 8.8: **BER remains nearly constant for various ambient lighting conditions and tick frequencies, with a target value of** 255

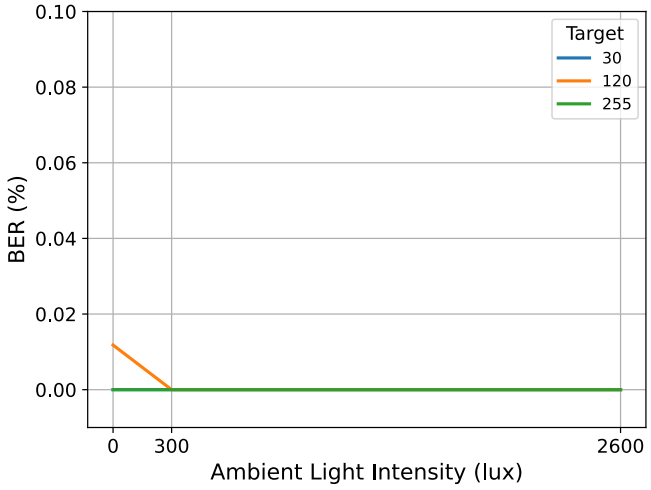

Figure 8.9: **BER remains nearly constant for various ambient lighting conditions and target values, with a tick frequency of 9kHz** ***(The curves for targets*** 30 ***and*** 255 ***nearly coincide)***

Regardless of the lighting intensity or variations in ambient lighting conditions, the system maintains a consistent BER. This can be attributed to the use of relative samples (refer section 5.2), which already have the effect of ambient lighting subtracted from them. Similar to the observations in subsection 8.3.3, the effect of ambient lighting on various frequencies and target values was also similar. As a result, the throughput was observed to be dependent only on the

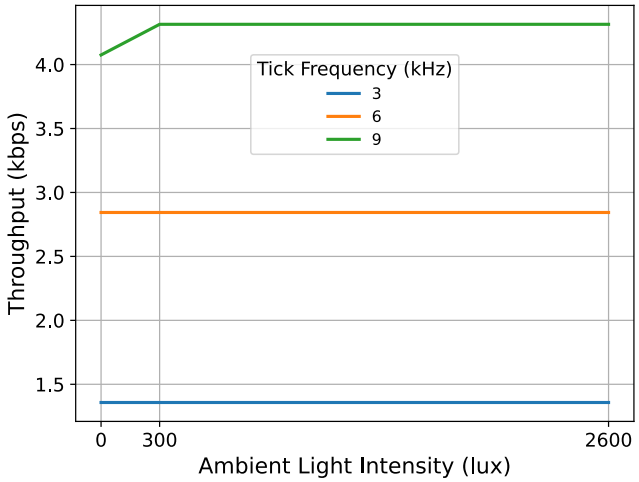

Figure 8.10: **Throughput is independent of the ambient lighting conditions for various tick frequencies and a target value of** 255

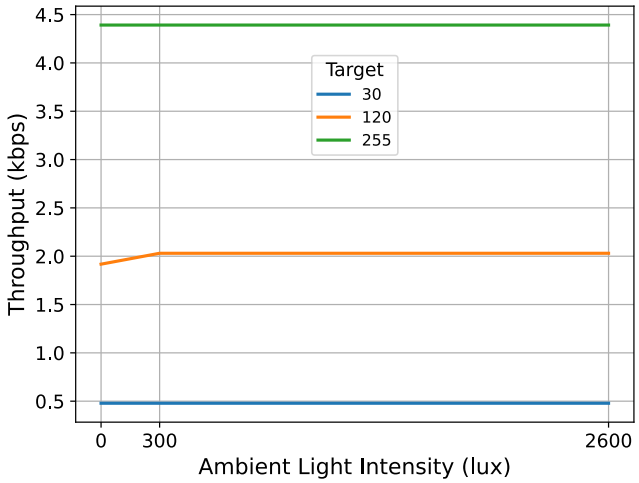

Figure 8.11: **Throughput is independent of the ambient lighting conditions for various target values and a tick frequency of 9kHz**

tick frequency (Figure 8.10) and target values (Figure 8.10), and not on the ambient lighting conditions.

8.3.4 Number of transmitters

Finally, the performance of the system under a varying number of transmitters was evaluated. To study the benefits of using multiple transmitters, each trans-

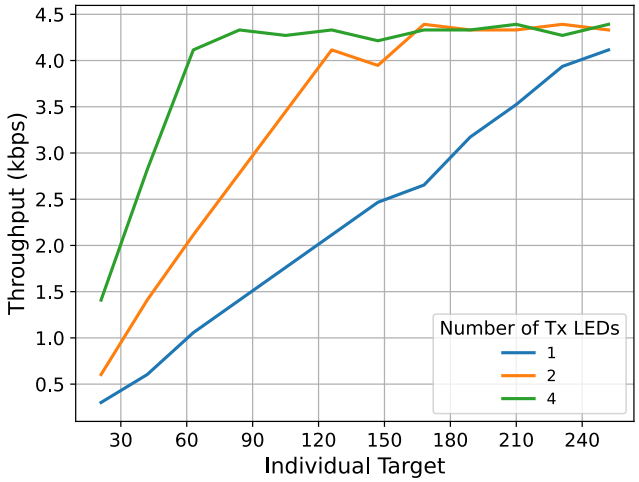

Figure 8.12: **At lower individual targets, the advantage of using multiple Tx LEDs is greater than that at higher individual target values**

mitter in the set was assigned the same target value, and this individual target value was chosen as the dependent variable, instead of the collective target value. For a particular collective target, the throughput is independent of the number of transmitters. The collective target value, hence, is not a suitable variable for investigating the effects of using multiple Tx LEDs. On the other hand, when the individual target value is considered, the collective target, and hence, the throughput depends on the number of transmitters. Hence, configurations with 1, 2, and 4 Tx LEDs with a tick frequency of 9kHz and varying individual target values, were studied. The results are displayed in Figure 8.12. It was observed that for lower individual targets, additional transmitters provided a significant throughput benefit. However, after a certain point, the throughput in the case of multiple Tx LEDs stagnated and the advantage over using a single Tx LED started reducing. This is because the collective target value is capped at 255. As the individual target value approaches 255, there remains a lesser scope for improvement in throughput, by including an additional transmitter. The results also showed that as the number of Tx LEDs increased, the stagnation was attained at lesser individual target values. Thus, further increasing the number of Tx LEDs will provide performance increment over a smaller range of individual targets. Increasing the number of Tx LEDs from 1 to 2, improved the throughput for a large range of individual targets. But increasing them to 2 to 4 provides an improvement in a much smaller range. Therefore, a large number of transmitters will not provide a huge throughput increment over the entire range of individual target values.

Chapter 9

Conclusions

In conclusion, this VLC system, comprising a 4x4 RGB LED display is capable of transmitting and receiving data using its pixels, without a noticeable degradation in the pixel appearance. This opens up possibilities for integrating data transfer capabilities in various existing and future applications, including information display units, signage, and microLED displays. The bidirectional functionality enables interactive and dynamic communication scenarios, fostering engagement and responsiveness.

The following are the key traits of the Screen Antenna system:

1. A maximum throughput of 4.4 kilobits per second can be achieved with a Bit Error Rate of less than 0.01%.

2. Communication is unaffected by the ambient light provided that the lighting conditions remain similar throughout the duration of the communication.

3. By tuning the Rx threshold parameter, the system can be operated at multiple Rx-Tx distances. Reliable communication is possible up to a distance of 20cm. This range can be increased slightly by increasing the feedback resistance of the transimpedance amplifier.

4. The peripheral circuitry and software modules are designed with the objective of scalability. However, the processing capabilities of the current system may hinder the expansion to large displays.

5. An Rx LED is able to receive data from some of the Tx LEDs that are not situated along the normal. While this has been used for many-to-one communication, it also means that perfect lateral alignment between the two displays is not necessary. The system can perform consistently with some amount of lateral shift. Depending on the distance, a slight rotational misalignment will also not pose a problem. Due to the dynamic nature of the system, in case of a misaligned configuration, the potential Tx set for a particular Rx will be automatically selected during the initial scanning phase.

6. Since the receiver expects the same target value for the entire message, it is not possible to change the red channel intensity of Tx LEDs until the

message transfer is complete. Thus the refresh rate of the red component of transmitting pixels is limited.

7. With the colour augmentation technique, a pixel is able to send data while displaying any colour. Even when the red component of the desired colour is zero, the Tx LED is able to send data, albeit at a lower rate. In such a case where the targets of individual Tx LEDs are small, the throughput can be significantly augmented by using multiple Tx LEDs in conjunction.

By employing visible light as the medium, the VLC system can take advantage of the vast available spectrum, avoiding congestion and interference commonly associated with radio frequency-based communication systems. This offers a reliable and secure communication channel, particularly in environments where other wireless technologies may be prone to interference or pose security concerns. Overall, the Screen Antenna presents a promising solution for efficient and flexible communication.

Chapter 10

Future Work

This successful implementation of the Screen Antenna prototype has generated several potential avenues for further development and exploration. These are listed in the sections below.

10.1 Signal Edge Detection at the Receiver

Instead of the level detection of the received signal, which is currently used, the edges can be detected instead (as presented in [16]). The transmitter and receiver can be synchronized such that the edges of the Manchester symbols fall within the sampling interval of the receiver. This offers a solution to two of the current limitations:

1. When an edge is detected, based on whether it is a positive or negative edge, the bit can be decoded as '1' or '0' respectively. When no edge is detected within the sampling interval, this indicates that the slot is inactive. Thus, a static target value is not needed by the receiver for detecting inactive slots. This also means that the red channel intensity of the transmitter LEDs does not have to be consistent during the transfer of the message, and hence, higher refresh rates are possible.

2. Signals edges, unlike the signal levels are not affected by the ambient conditions. For edge detection, initial sampling of ambient light is not necessary. And mainly, the data transfer is not hindered if the ambient conditions change during the message transfer. Of course, a change in lighting will introduce a false edge in the transmitted signal, but this will only cause a single decoding error, as the system continues to decode the subsequent bits correctly.

10.2 Spatial and Temporal Colour Difference

In the current system, the colour augmentation technique takes into account the instantaneous colour of a particular pixel alone. The perceived colour difference is considered to be independent of the colours emitted by other pixels, and also of the changes in the colour over time. However, in reality, this is not

how the human vision interprets information. The human perception exhibits a "blur"-property [27], whereby the colour perceived for a particular pixel is also affected by the colours of the neighbouring pixels. Moreover, for a display, in most circumstances, the pixel colour is continuously changing. The human brain processes changing colours differently than static colours. With human cognition depending on more factors than just the pixel colour, it could be possible to enhance the colour augmentation technique and extract a greater throughput out of the system. Existing works such as Zhang et al. [2010], Tong et al. [1999] and Kaya et al. [2011] aim at extending the *CIELAB* colour space to images (instead of a single pixel) and videos, and developing a metric to evaluate the colour difference in spatial and temporal domains. These methods are computationally expensive, and due to the large number of possible combinations involved, it is difficult to derive approximation functions such as the ones currently in use. However, with a more high-performance processing unit, there exists significant scope for studying the effects of incorporating the spatial and temporal colour difference concept into the system.

10.3 Multi-core Setup

For larger displays, the processor will have to manage a greater number of pixels. This calls for an increased processing speed. However, increasing the processing speed is itself not sufficient, since the I^2C and SPI transaction times are still the bottlenecks. For a larger display, with a larger number of LED Drivers and ADCs, there will be a significant lag between the operations for the first and last pixel. Thus some parallelism needs to be introduced to perform multiple I^2C and SPI transactions in parallel. This opens up possibilities for investigating the performance of various multi-core architectures with the Screen Antenna system. Furthermore, parallelism can also unveil prospects for multi-channel channel communication, including full-duplex communication between the two displays.

10.4 ASIC

The I^2C transaction bottlenecks exist because the PWM is handled by the microcontroller instead of the LED Driver IC. At every PWM level change, the microcontroller sends commands to the LED Driver to change the state of the LED. Such a system is implemented for two reasons:

1. Reliable communication requires a tick frequency of 9kHz, but the PWM frequency of the LED Driver IC cannot be lowered to this order.

2. Data is transmitted using Manchester coding and the LED Driver cannot be configured to modulate the PWM signal with Manchester symbols

Thus it could be beneficial, in terms of speed, to implement some of the software functionality in hardware. A peripheral Application-Specific IC (ASIC) design could enhance the scalability and performance of the system. By implementing some configurability such as the selection of Tx sets in the peripheral ASIC, the dependence of the system on microcontroller's software operation can be reduced.

Bibliography

[1] Hisham Abuella, Mohammed Elamassie, Murat Uysal, Zhengyuan Xu, Erchin Serpedin, Khalid A. Qaraqe, and Sabit Ekin. Hybrid rf/vlc systems: A comprehensive survey on network topologies, performance analyses, applications, and future directions. *IEEE Access*, 9:160402–160436, 2021. doi: 10.1109/ACCESS.2021.3129154.

[2] Aishwarya Choorakuzhiyil and Neha Tiwari. Promising candidature of oleds, mini leds & micro leds in the realm of ar/vr applications. In *2022 International Conference on Smart Generation Computing, Communication and Networking (SMART GENCON)*, pages 1–7, 2022. doi: 10.1109/SMARTGENCON56628.2022.10083915.

[3] Hyunchae Chun, Sujan Rajbhandari, Grahame Faulkner, Dobroslav Tsonev, Harald Haas, and Dominic O'Brien. Demonstration of a bidirectional visible light communication with an overall sum-rate of 110 mb/s using leds as emitter and detector. In *2014 IEEE Photonics Conference*, pages 132–133, 2014. doi: 10.1109/IPCon.2014.6995247.

[4] Kai-Cheng Chung, Jia-Jyun Lee, Jia-Rui Huang, Yan-Jiun Lai, Ke-Horng Chen, Ying-Hsi Lin, Shian-Ru Lin, and Tsung-Yen Tsai. A dynamic compensated and 95% high-efficiency supply buffer in rgb virtual pixel microled display for reducing ghosting by 73% and achieving four times screen resolution. *IEEE Transactions on Power Electronics*, 36(7):8291–8299, 2021. doi: 10.1109/TPEL.2020.3047372.

[5] TE Connectivity. Photodiode Sensors, 2020. URL `https://www.te.com/usa-en/products/sensors/optical-sensors/photodiode-sensors.html`.

[6] Paul Dietz, William Yerazunis, and Darren Leigh. Very low-cost sensing and communication using bidirectional leds. In Anind K. Dey, Albrecht Schmidt, and Joseph F. McCarthy, editors, *UbiComp 2003: Ubiquitous Computing*, pages 175–191, Berlin, Heidelberg, 2003. Springer Berlin Heidelberg. ISBN 978-3-540-39653-6.

[7] eBay Inc. Hamamatsu R300 Photomultiplier Tube, 2023. URL `https://www.ebay.com/itm/294174233684`.

[8] Mohamed I. Gabr. Data transmission via visible light communication (vlc) technique. *International Journal of Innovative Research in Science, Engineering and Technology*, 5:16473–16481, 09 2016. doi: 10.15680/IJIRSET.2016.0509133.

[9] J. L. Henao, N. Guerrero González, and J. C. García-Álvarez. Three-dimensional spatial coding based on hybrid pulse width and pulse position modulation for simultaneous data transmission and brightness control on rgb led arrays. In *2019 IEEE Colombian Conference on Communications and Computing (COLCOM)*, pages 1–6, 2019. doi: 10.1109/ColComCon.2019.8809151.

[10] J. L. Henao-Rios, D. Marquez-Viloria, and N. Guerrero-González. Real time implementation of a hybrid differential manchester-pwm encoding for constant data rate under variable brightness in vlc systems. In *2020 IEEE Colombian Conference on Communications and Computing (COLCOM)*, pages 1–5, 2020. doi: 10.1109/COLCOM50121.2020.9219756.

[11] Christoph Hönck. Design of a Touch Screen Using Only an LED Matrix. 2011. URL `https://diglib.tugraz.at/design-of-a-touch-screen-using-only-an-led-matrix-2011`.

[12] Sindhubala Kadirvelu and Vijayalakshmi B. Visible light communication using led as receiver with the effect of ambient light. *Optical and Quantum Electronics*, 50, 12 2017. doi: 10.1007/s11082-017-1280-4.

[13] Sertan Kaya, Travis Bennett, Mariofanna Milanova, John Talburt, Brian Tsou, Marina Altynova, and Hongyan Xu. Perception-based image/video quality metric using CIELAB color space. In Edward M. Carapezza, editor, *Sensors, and Command, Control, Communications, and Intelligence (C3I) Technologies for Homeland Security and Homeland Defense X*, volume 8019, page 801908. International Society for Optics and Photonics, SPIE, 2011. doi: 10.1117/12.883682. URL `https://doi.org/10.1117/12.883682`.

[14] Latif U. Khan. Visible light communication: Applications, architecture, standardization and research challenges. *Digital Communications and Networks*, 3, 05 2017. doi: 10.1016/j.dcan.2016.07.004.

[15] Bernhard Kramer. *Advances in Solid State Physics*. Springer Science & Business Media, September 2003. ISBN 978-3-540-40150-6. Google-Books-ID: oREQToB2q2UC.

[16] Shuai Li, Ashish Pandharipande, and Frans M. J. Willems. Adaptive visible light communication led receiver. In *2017 IEEE SENSORS*, pages 1–3, 2017. doi: 10.1109/ICSENS.2017.8234237.

[17] Muhammad Sarmad Mir, Behnaz Majlesein, Borja Genoves Guzman, Julio Rufo, and Domenico Giustiniano. Rgb led bulbs for communication, harvesting and sensing. In *2022 IEEE International Conference on Pervasive Computing and Communications (PerCom)*, pages 180–186, 2022. doi: 10.1109/PerCom53586.2022.9762392.

[18] *PCA9956B - 24-channel Fm+ I2C-bus 57 mA/20 V constant current LED driver*. NXP, 2020. URL `https://www.nxp.com/docs/en/data-sheet/PCA9956B.pdf`.

[19] Digital Photography Review. Canon is now selling CMOS image sensors, including a 120MP APS-H beast, 2018. URL https://www.dpreview.com/news/0671207908/canon-is-now-selling-cmos-image-sensors-including-a-120mp-aps-h-beast.

[20] Rohail Sarwar, Bin Sun, Meiwei Kong, Tariq Ali, Chuying Yu, Bo Cong, and Jing Xu. Visible light communication using a solar-panel receiver. In *2017 16th International Conference on Optical Communications and Networks (ICOCN)*, pages 1–3, 2017. doi: 10.1109/ICOCN.2017.8121577.

[21] Stefan Schmid, Giorgio Corbellini, Stefan Mangold, and Thomas R. Gross. Led-to-led visible light communication networks. In *Proceedings of the Fourteenth ACM International Symposium on Mobile Ad Hoc Networking and Computing*, MobiHoc '13, page 1–10, New York, NY, USA, 2013. Association for Computing Machinery. ISBN 9781450321938. doi: 10.1145/2491288.2491293. URL https://doi-org.tudelft.idm.oclc.org/10.1145/2491288.2491293.

[22] MB Solartechniek. Solar Panel 500w, January 2020. URL https://mbsolar.nl/index.php/product/solar-panel-500w-2/.

[23] G. Stepniak, M. Kowalczyk, L. Maksymiuk, and J. Siuzdak. Transmission beyond 100 mbit/s using led both as a transmitter and receiver. *IEEE Photonics Technology Letters*, 27(19):2067–2070, 2015. doi: 10.1109/LPT.2015.2451006.

[24] TinyTronics. RGB LED - 5mm Bright - Common Cathode, 2023. URL https://www.tinytronics.nl/shop/en/components/leds/leds/rgb-led-5mm-bright-common-cathode.

[25] Xin Tong, David J. Heeger, and Christian J. Van den Branden Lambrecht. Video quality evaluation using ST-CIELAB. In Bernice E. Rogowitz and Thrasyvoulos N. Pappas, editors, *Human Vision and Electronic Imaging IV*, volume 3644, pages 185 – 196. International Society for Optics and Photonics, SPIE, 1999. doi: 10.1117/12.348439. URL https://doi.org/10.1117/12.348439.

[26] Fahim Aziz Umrani, Faisal Ahmed Dahri, Abdul Waheed Umrani, and Hyder Bux Mangrio. The internet of led: Indoor visible light communication using led as transmitter and receiver. In *2018 21st International Symposium on Wireless Personal Multimedia Communications (WPMC)*, pages 75–78, 2018. doi: 10.1109/WPMC.2018.8712906.

[27] Erhu Zhang, Yajun Chen, Jia Yu, and Yang Yang. A study of image color quality evaluation based on s-cielab. In *2010 3rd International Congress on Image and Signal Processing*, volume 3, pages 1110–1114, 2010. doi: 10.1109/CISP.2010.5646866.

[28] Klaas Minne Van Der Zwaag, Marianne Pontara Marinho, Wesley Da Silva Costa, Francisco De Assis Souza Dos Santos, Teodiano Freire Bastos-Filho, Helder R. O. Rocha, Marcelo E. V. Segatto, and Jair A. L. Silva. A manchester-ook visible light communication system for patient monitoring in intensive care units. *IEEE Access*, 9:104217–104226, 2021. doi: 10.1109/ACCESS.2021.3099462.

Appendix A

Circuit Schematics for a Single Row of 4 LEDs

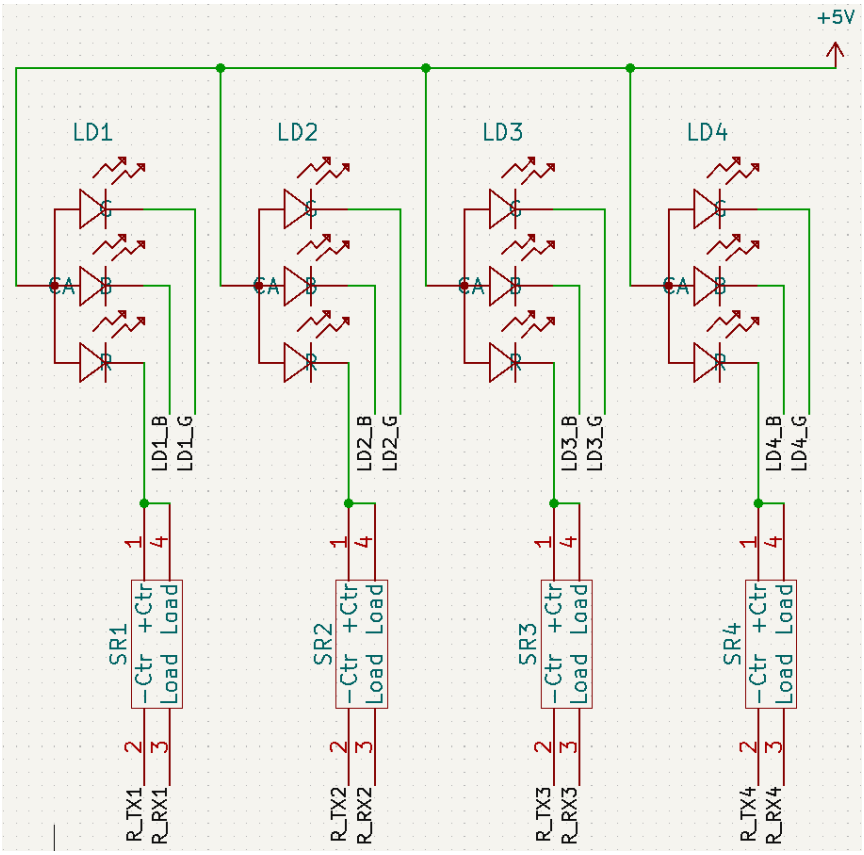

Figure A.1: **LEDs and associated Solid-state Relays**

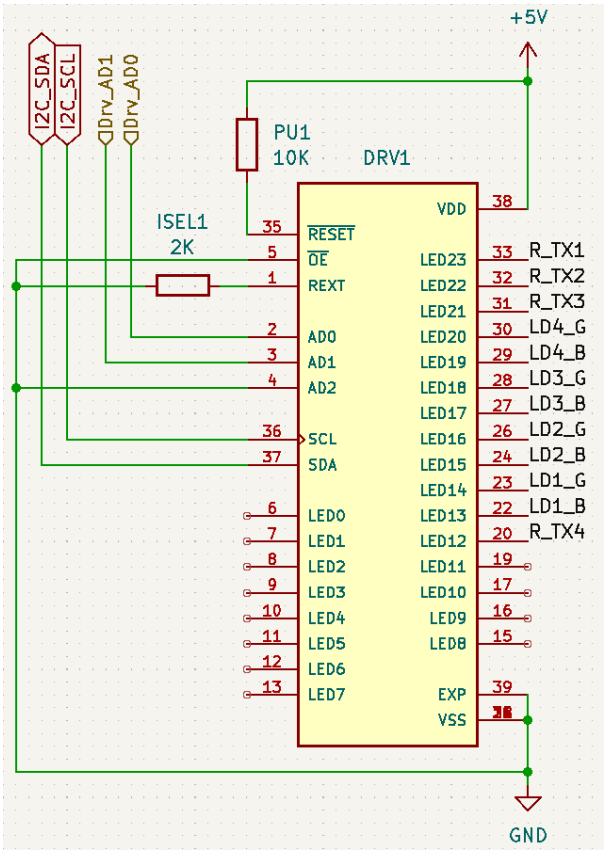

Figure A.2: **LED Driver**

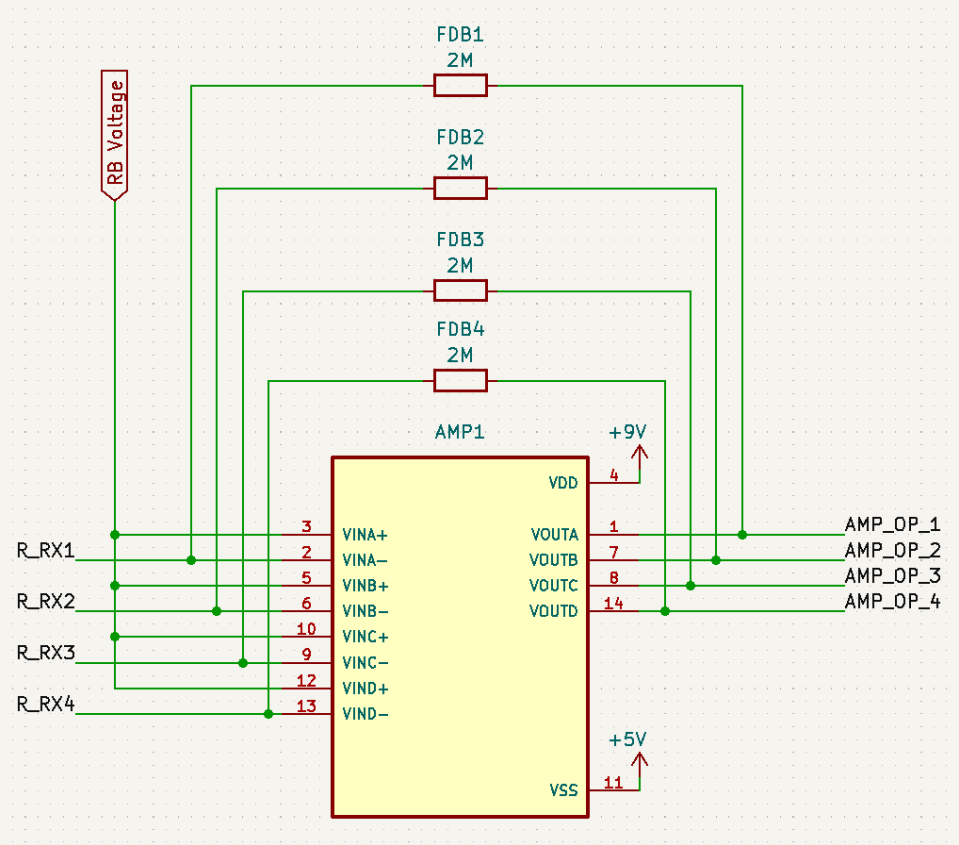

Figure A.3: **Transimpedance Amplifier**

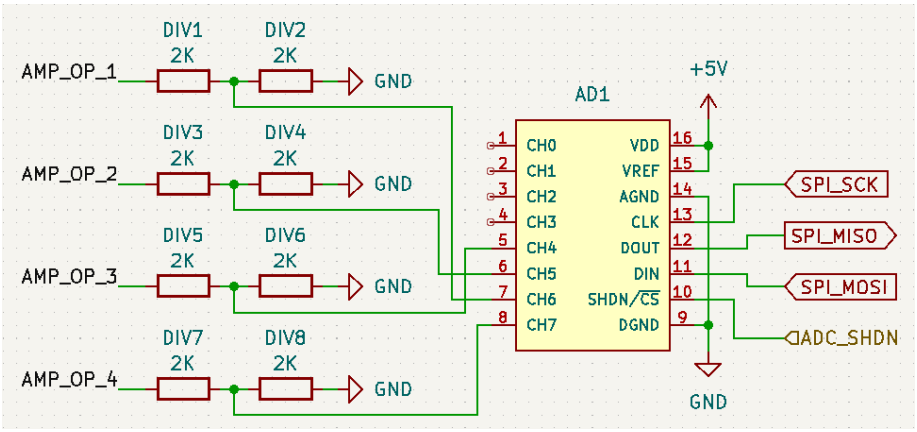

Figure A.4: **Analog to Digital Converter (ADC)**

Appendix B

PCB Designs

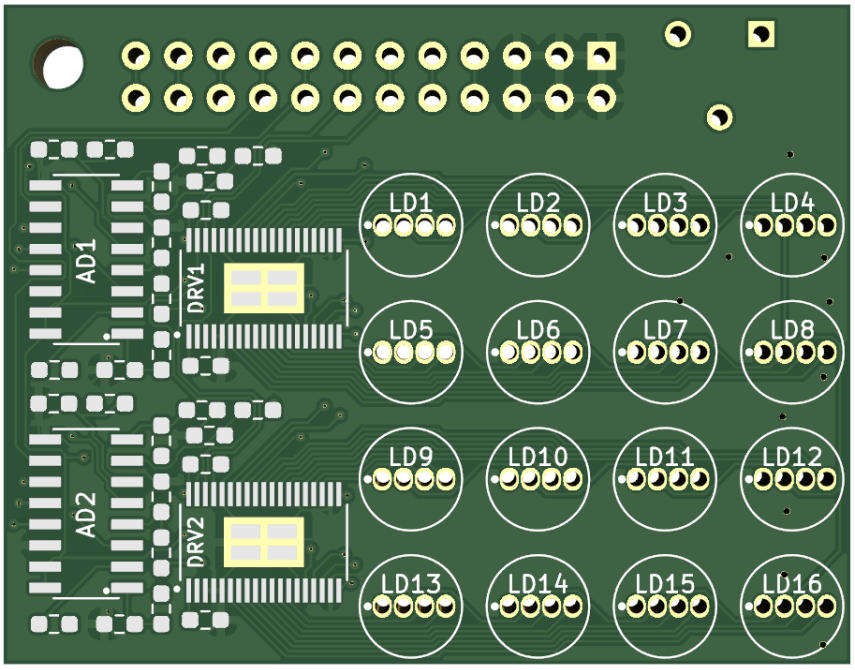

Figure B.1: **PCB Front View (without components)**

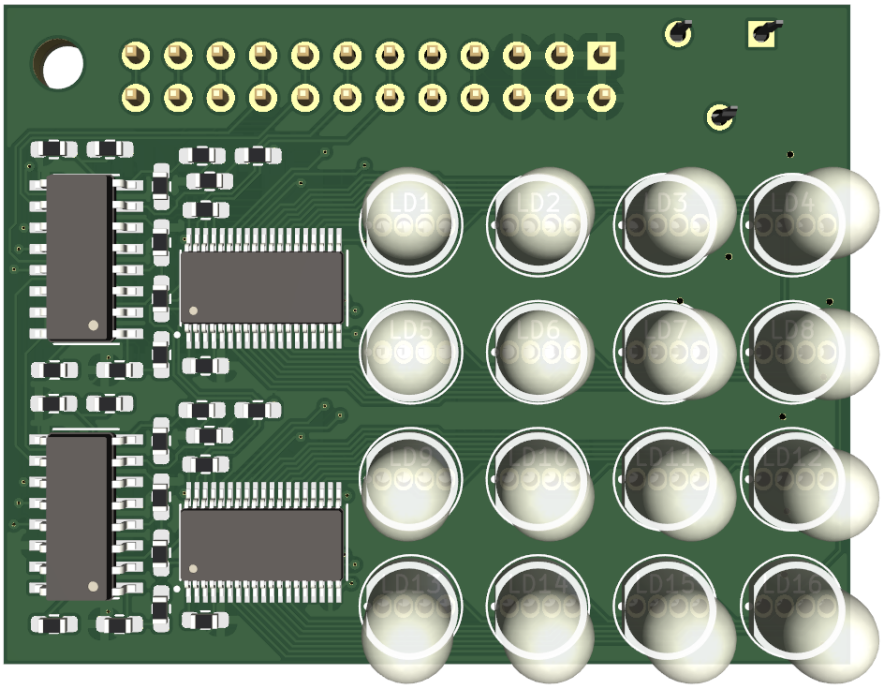

Figure B.2: **PCB Front View (with components)**

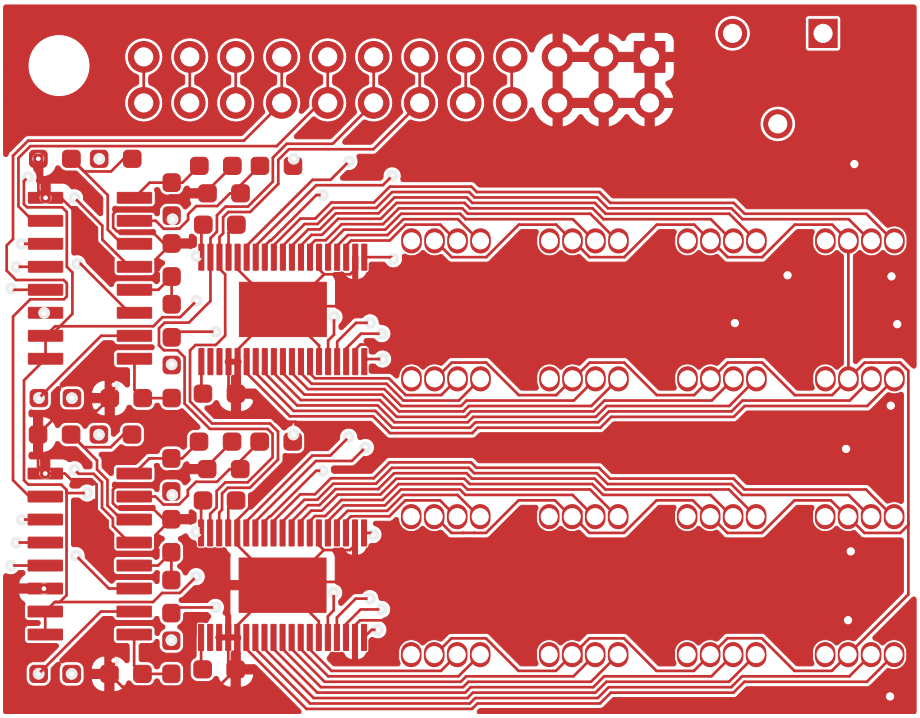

Figure B.3: **PCB Front Routing**

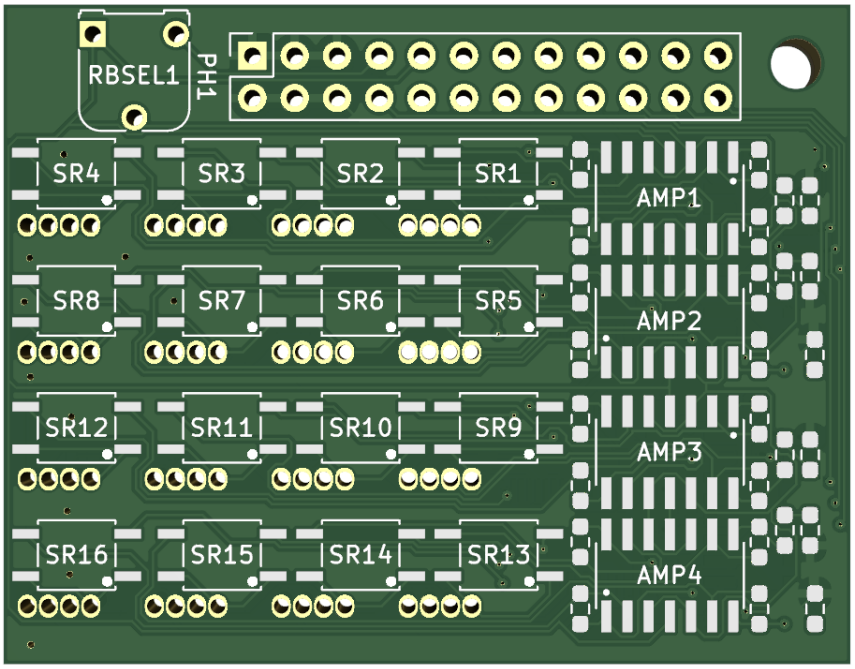

Figure B.4: **PCB Back View (without components)**

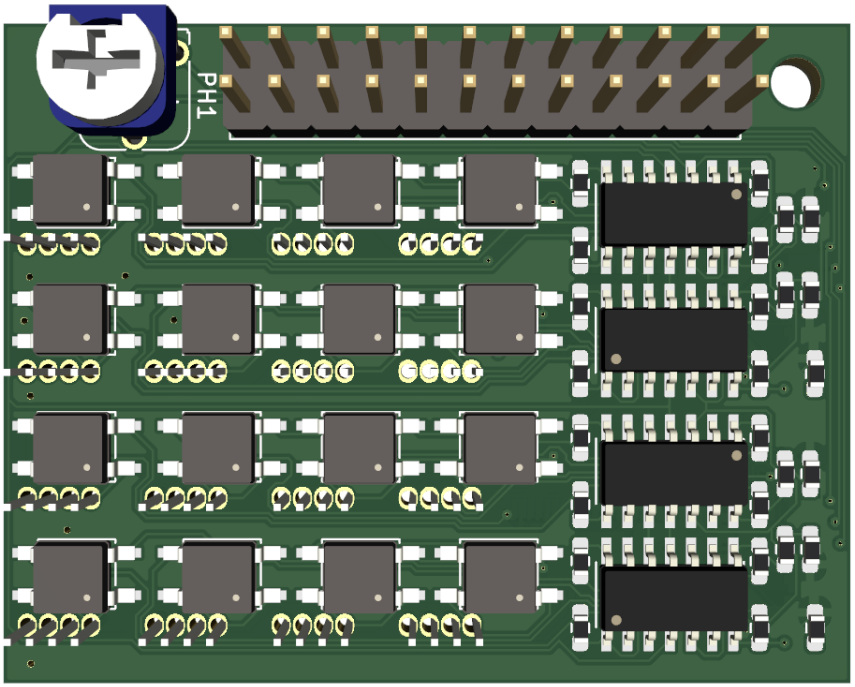

Figure B.5: **PCB Back View (with components)**

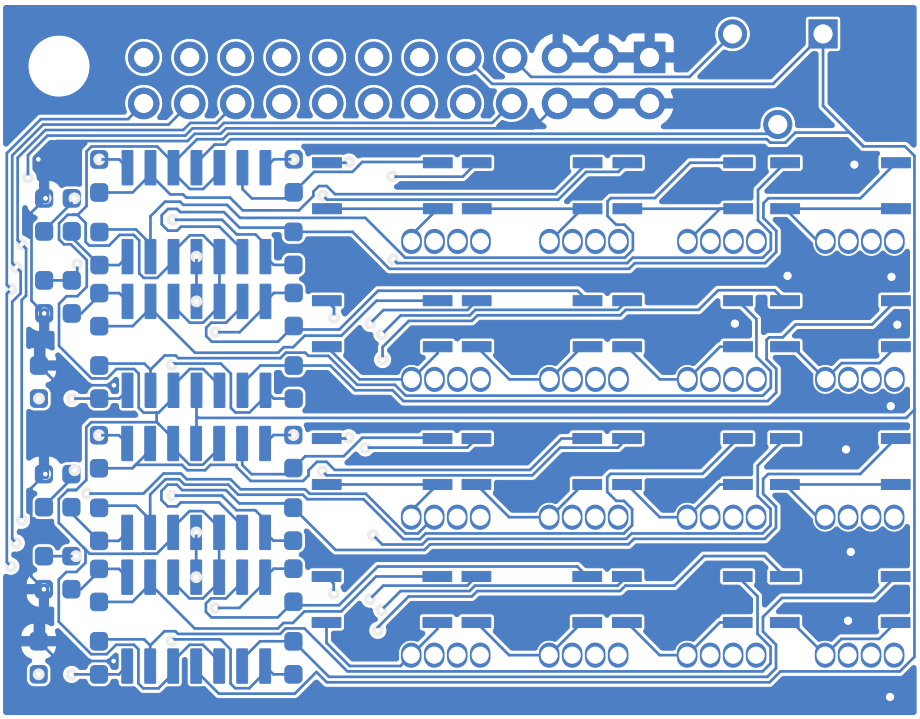

Figure B.6: **PCB Back Routing**